Article:

Neal, J, Bates, P, Villanueva, I et al. (3 more authors) (2012) How much physical complexity is needed to model flood inundation? Hydrological Processes, 26 (15). 2264 - 2282. ISSN 0885-6087

https://doi.org/10.1002/hyp.8339

How much physical complexity is needed to model flood inundation?

Jeffrey Neal[1*], Ignacio Villanueva[2], Nigel Wright[3], Thomas Willis[3], Timothy Fewtrell[4] and Paul Bates[1]

[1]School of Geographical Sciences, University of Bristol, Bristol. BS8 1SS. UK,
[2]Ofiteco Ltd., Avenida de Portugal, 81. 28071, Madrid. Spain.
[3]School of Civil Engineering, University of Leeds, Leeds. LS2 9JT. UK
[4]Willis Research Network, Willis Re, Willis Building, 51 Lime Street, London. EC3M 7DQ. UK

* Corresponding author. Tel.: +44 (0)117 92 88290; fax: +44 (0)117 928 7878
E-mail address: j.neal@bristol.ac.uk

Abstract

Two-dimensional flood inundation models are widely used tools for flood hazard mapping and an essential component of statutory flood risk management guidelines in many countries. Yet we still don't know how much physically complexity a flood inundation model needs for a given problem. Here, three two-dimensional explicit hydraulic models, that can be broadly defined as simulating diffusive, inertial or shallow water waves, have been benchmarked using test cases from a recent Environment Agency for England and Wales (EA) study, where results from industry models are also available. To ensure consistency the three models were written in the same code and share subroutines for all but the momentum (flow) and time stepping calculations. The diffusive type model required much longer simulation times that the other models, whilst the inertia model was the quickest. For flows that vary gradually in time, differences in simulated velocities and depths due to physical complexity were within 10% of the simulations from a range of industry models. Therefore, for flows that vary gradually in time it appears unnecessary to solve the full two-dimensional shallow water equations. As expected however, the simpler models were unable to simulate supercritical flows accurately. Finally, implications of the results for future model benchmarking studies are discussed in light of a number of subtle factors that were found to cause significant differences in simulations relative to the choice of model.

Keywords: Hydraulic modelling, Benchmarking, flood inundation, physical complexity, simple models

1 Introduction

Two-dimensional flood inundation models are widely used tools for flood hazard mapping and an essential component of statutory flood risk management guidelines in many countries. For both industry and research applications there are a wide variety of shallow water codes that account for varying degrees of physical complexity and offer subtly different solutions to a given problem. Understanding the potential differences between these codes for industry applications was a key driver of recent two-dimensional model benchmarking reports commissioned by the Environment Agency for England and Wales (Crowder et al., 2004; Néelz and Pender, 2010) to aid procurement decisions and maintain standards.

Previous model benchmarking studies have usually tracked the development of new numerical methods or the adoption of new techniques as the necessary data or computational resources become available. For example, the increasing use of two-dimensional models over one-dimensional models during the past decade has been partly driven by developments in digital elevation modelling (DEM's), especially from airborne LiDAR data (Cobby et al., 2001). Thus, as the capability has developed it has been necessary to better understand the effects of moving to two-dimensions given different applications. Comparisons between one-dimensional, two-dimensional and coupled one-two dimensional river modelling approaches (e.g. Horritt and Bates (2002); Werner (2004) and Tayefi et al. (2007)) have highlighted conceptual problems with the one-dimensional approach applied to overbank flows when compared to the sometimes complex flow pathways simulated by two-dimensional models. Leopardi et al. (2002) includes a more extensive review of benchmarking studies on coupled 1D and 2D codes from the 1990's.

Benchmarking studies will often take newly developed or simplified models and compare them to more established or complex models. Such work is usually motivated by the computational cost of many two-dimensional model codes, which still restricts the use of hydraulic models models within Monte Carlo frameworks, despite continued advances in computer hardware (Neal et al., 2010; Lamb et al., 2010). The significant cost associated with each simulation has maintained interest in techniques that can approximate simulations from full two-dimensional shallow water models with less computation. Recent examples include porosity based methods for representing sub-grid scale features in coarse resolution models (Guinot and Soares-Frazao, 2006; Yu and Lane, 2006; McMillan and Brasington, 2007,) methods without momentum such as volume spreading (Hall et al., 2003; Gouldby et al., 2008), models that consider inertia and diffusion but ignore advection (Aronica et al., 1998; Bates et al., 2010), diffusive models (Prestininzi et al., 2009) and emulators (Hall et al., 2011). Bates and De Roo (2000) and Horritt and Bates, (2001) compared a storage cell approximation of a diffusion wave with an unstructured finite element model of a rural river and floodplain. Differences were noted between the models, particularly regarding the ability of the storage cell model to predict wave speed, which was later improved upon by Hunter et al. (2005) through the implementation of an adaptive time-step constraint. However, the models considered by Bates and De Roo (2000) and Horritt and Bates (2001) simulated similar inundation extents in that differences were less than the expected errors in the remotely sensed data used to evaluate the models at that time. Lack of observation data turned out to be a common problem when moving from purely comparing model simulations to evaluating model accuracy for spatially distributed real world events at and above the reach scale (e.g. Horritt et al., 2000; Mignot et al., 2006; Werner et al., 2005; Neal et al., 2009).

Other studies have looked at benchmarking alternative two-dimensional shallow water models (e.g. Horritt, 2007), where recent work has focused on urban settings because the risks are typically greater than in rural areas and the availability of DEM data perceived as fit for purpose has been increasing (Fewtrell, 2011). Hunter et al. (2008) compared three full shallow water codes (Syme, 1991; Villanueva and Wright, 2006, Liang et al., 2006) and two diffusive codes (Bradbrook et al., 2004; Hunter et al., 2005) for an urban test site in Glasgow, UK. They found differences in the depth and extent dynamics given the range of physical process representations and numerical solvers tested, although the significance of these given uncertainty in factors such as inflow discharges and surface friction is an ongoing debate within the community. This test case was subsequently used to evaluate mesh generation techniques (Schubert et al., 2008), grid resolution effects (Fewtrell et al., 2008), methods of parallelising models (Neal et al., 2010) and uncertainty in the magnitude of flow for given rainfall return periods (Aronica et al., submitted).

Néelz and Pender (2010) benchmarked the majority of industry codes used for flood risk modelling in the UK by the Environment Agency and commercial consultants. The industry codes (including: ISIS2D, SOBEK, TUFLOW, MIKEFLOOD, InfoWorks2D, Flowroute & JFLOW-GPU) were required to simulate velocity and depth dynamics across the range test cases listed in Table 1, which were designed to cover most statutory flood risk modelling requirements in the UK. In this paper, three physical process representations of floodplain flow, described in the next section, will be benchmarked using four of the test cases from this study identified in Table 1.

One of the key issues when comparing industry codes is the difficulty in achieving suitable consistency between test case implementations. Without this there is significant uncertainty in the cause of simulation differences, meaning discrepancies between results cannot be attributed to a narrow enough range of factors to allow useful conclusions to be drawn. Differences in how modellers interpret the same test case are the easiest to avoid by using a single code where the state variables of each 'model' (elevation, inflow etc) can be taken from a shared environment. This also means model parameters will be sourced and manipulated in a consistent manner (e.g. in the model used here the roughness across a cell edge is a linear interpolation of the roughness attributed to each neighbouring grid cell). This degree of constancy can be assumed between models in different codes but is not easily verified without extensive analysis of the source code, which for commercial confidentiality reasons may not be available. Treatment of wetting and drying, wet to dry edges, friction and source terms, inflows and normal depth boundaries may also differ subtly between codes, both in terms of approach and parameterisation. All of these factors may alter simulation results before any consideration of numerical scheme and physical complexity is taken into account, adding significant uncertainty to any discussion.

To address this issue the models in this study were written within a single code ensuring a level of constancy between model state variables and parameters that was not possible in the studies presented above. The models used were the full shallow water model LISFLOOD-Roe based on the TRENT model (Villanueva and Wright, 2006), an inertial wave model LISFLOOD-ACC (Bates et al., 2010) that represents a simplified shallow water wave and a diffusion wave model LISFLOOD-ATS (Hunter et al., 2005). These all form part of the single LISFLOOD-FP code. Results from the industry models in Néelz and Pender (2010) have been used to provide context to the LISFLOOD-FP simulations, especially in regard to the magnitude of difference between the simpler and full shallow water models. A key interest not covered by previous studies will be the ability of the simpler models to simulate velocity and therefore flood hazard, along with the sensitivity to some often hidden coding and parameterisation decisions. Results are discussed under two sections. The first deals with the inter-comparison of the three models and their response to each test, from which, conclusions regarding the necessary physical complexity for each test are drawn. The second section discusses the implications of these results for the Environment Agency model benchmarking study and implications for model benchmarking best practice.

2 Models

This benchmarking exercise focuses on three two-dimensional hydraulic models within the LISFLOOD-FP code. Each model is a module within the code that is activated by a key word in the model parameter file prior to simulation. Once initialised, all models utilise the same input files and data structures, along with many shared subroutines. In fact, as the continuity equation is the same for all models they only differ in respect of the flow equation and time stepping. The models were chosen to cover a typical range of physical complexities based on the shallow water equations or simplifications of them. The three models (LISFLOOD-Roe, LISFLOOD-ACC and LISFLOOD-ATS) are summarised in Table 2 and described in the following section.

LISFLOOD-Roe is the two-dimensional shallow water model from Villanueva and Wright (2006), thus it calculates the flow according to the complete Saint Venant formulation. The method is based on the Godunov approach and uses an approximate Riemann solver by Roe (Roe, 1981). The explicit discretisation is first-order in space on a raster grid. It solves the full shallow water equations with a shock capturing scheme. LISFLOOD-Roe uses a point-wise friction based on the Manning´s equation, while the domain boundary/internal boundary (wall) uses the ghost cell approach. The stability of this approach is approximated by the CFL condition for shallow water models, which is shown in Table 2. As the complete model formulation is quite lengthy and relatively well known it is not reproduced here.

LISFLOOD-ACC is a one-dimensional inertial model (e.g. advection is ignored), and hence is decoupled in x and y directions for two-dimensional simulation over a raster grid. The method is first-order in space and explicit in time, but uses a semi-implicit treatment for the friction term to aid stability (See Bates et al., 2010). To calculate the flow between cells the equation derived by Bates et al. (2010) is implemented:

$$Q^{t+\Delta t} = \frac{q^t - g h^t_{flow} \Delta t \frac{\Delta(h^t + z)}{\Delta x}}{\left(1 + g h^t_{flow} \Delta t n^2 |q^t| \Big/ \left(h^t_{flow}\right)^{\frac{10}{3}}\right)} \Delta x$$

where g is the acceleration due to gravity (ms^{-1}), n is Manning's roughness coefficient($sm^{-1/3}$), h is depth (m) and z is cell elevation (m) such that $\Delta(h^t + z)$ is the difference in water surface elevation between two cells (m), Δx is the cell resolution (m), Q is flow (m^3s^{-1}), q is water flux (m^2s^{-1}) and h^t_{flow} is the depth of flow between two cells (m) defined as the maximum water surface elevation in neighbouring cells minus the maximum bed elevation in neighbouring cells. This model formulation was used previously by Neal et al. (2011) under the name LISFLOOD-INT. The stability of this approach is approximated by a modification to the CFL condition for shallow water models that neglects the velocity component as shown in Table 2.

LISFLOOD-ATS is a one-dimensional approximation of a diffusion wave based on uniform flow formula, which are decoupled in x and y directions (Bates and de Roo, 2000). Manning's equation, as shown below, is implemented explicitly on a raster grid as described in detail by Hunter et al. (2005a):

$$Q^{t+\Delta t} = \frac{\left(h^t_{flow}\right)^{\frac{5}{3}}}{n} \left(\frac{\Delta(h^t + z)}{\Delta x}\right)^{\frac{1}{2}} \Delta x$$

LISFLOOD-ATS should be very cheap to solve as it has the simplest physical representation, however its stable time-step has been shown to be significantly smaller than that determined by the CFL condition (Bates et al., 2010; Hunter et al., 2005) and is calculated by the equation in Table 2. This equation includes the water surface slope which causes the time-step will go to zero with a flat water surface, meaning a linearization of the time-step equation is needed at low slope to prevent the scheme stalling. The conditions under which this linearization is implemented are also summarised in Table 2.

As discharge between cells is calculated across each cell face, the continuity equation for the three models sums the flows across each face of every cell in the model and then multiplies by the time step to calculate a volume change, before dividing by the cell area to calculate a depth change for the cell.

Where available, simulation results will be presented from a range of industrial codes that were benchmarked on the test cases considered here as part of a recent Environment Agency benchmarking exercise (Néelz and Pender 2010). The EA benchmarking study included 14 models; however results from only six commercial programs will be presented here. The aim being to provide an industrial benchmark for the LISFLOOD-FP results rather than a comparison of all models. Of the six programs selected, four are full shallow water models broadly similar to LISFLOOD-Roe (TUFLOW (Syme, 1991), ISIS2D (Liang et al., 2006; 2007), Infoworks2D (Lhomme et al., 2010), SOBEK (Stelling, 1998)) and two are diffusive type models that are similar to LISFLOOD-ATS (JFLOW-GPU (Bradbrook et al., 2004; Lamb et al., 2010) and FlowRoute). There is no current industry implementation of the LISFLOOD-ACC algorithm.

3 Results

These results summarise findings from four of the ten EA test cases listed in Table 1. The reasons for not implementing all tests are as follows:

- Tests 1&2 were ignored to save space and because later test were assumed to be more difficult and evaluate similar properties.
- Test 6a is a higher resolution (laboratory scale) and lower friction version of 6b. It was not practical to apply either of the simpler models to this test given the results from test 6b.
- Tests 7, 8a & 8b were deemed outside the scope of this paper because they require 1D channel, rainfall and sewer models, respectively.

Before discussing the results from each test, simulation times are presented in Table 3 based on single core implementations of the model. Some of the simulation time differences between models were due to variations in the inundation dynamics between codes, particularly for test cases 3&6b where there was a larger variation in the number of wet cells. Simulated dynamics were more alike in tests 4&5 (see subsequent results sections) meaning the difference in simulation time between the models provides indicative data on their relative speeds. For test 4, which has the longest simulation time, LISFLOOD-Roe was 3.3 times slower than LISFLOOD-ACC and 116.2 times faster than LISFLOOD-ATS. These differences were not unexpected. For LISFLOOD-ATS, the time-step is proportional to $\frac{1}{\Delta x^2}$ rather than $\frac{1}{\Delta x}$ as is the case with the other models, whilst the inclusion of potentially very small water surface slopes in the time stepping equation (see Table 2) will further reduce the time-step relative to the other codes, especially if the computational grid is aligned with the water surface contours. Unlike LISFLOOD-ACC, LISFLOOD-Roe includes absolute velocity in the time stepping equation because advection is included in the model physics. Another indicator of potential computational efficiency is the relative number of non-integer power functions needed to calculate flow in each model, these are nine (LISFLOOD-Roe), one (LISFLOOD-ACC) and two (LISFLOOD-ATS). Thus, LISFLOOD-ACC requires a similar amount of computation per time step to LISFLOOD-ATS and significantly less computation per time-step than LISFLOOD-Roe. The relative simulation times vary between the test cases due to resolution, velocity, depth and slope factors, although in all but one case the rank order of the models in terms of simulation time was consistent. Note that all three LISFLOOD-FP models are explicit in time and that implicit schemes would allow longer time-steps to be used.

Mass balance errors for each model simulation are summarised in Table 4 using the cumulative volume error (m^3) at the end of each simulation, which is the sum of volume errors made by the model calculated at regular intervals through the simulation. Such that:

$$V_e = V^N - V^0 + \sum_{t=1}^{N} \Delta t^t Q^t_{in} - \sum_{t=1}^{N} \Delta t^t Q^t_{out}$$

where the volume error V_e over a period of N time-steps is the initial domain volume V^{t0} plus the sum of inflow volumes $\Delta t Q_{in}$ over each of the N time-steps minus the sum of outflow volumes from the domain $\Delta t Q_{out}$ minus the domain volume at the end of the N time-steps V^N. As all the test cases used here have closed boundaries at the edge of the domain the outflow volumes were zero. LISFLOOD-ATS tended to have the smallest volume errors and these were always several orders of magnitude below 1% of the domain volume. LISFLOOD-ACC either had the smallest or greatest mass error depending on the test case. Reasons for larger mass errors in LISFLOOD-ACC simulations of test case 3&6b and LISFLOOD-Roe simulations of tests 4&5 are discussed in subsequent test case specific sections.

3.1 Momentum conservation over a bump

This case is designed to test a code's ability to simulate flow down a slope and over a bump. It is test case 3 in the EA benchmarking study (Table 1) and includes a two metre resolution DEM re-sampled to five metres (Fig. 1) with a Manning's coefficient of 0.01. Water enters the domain along the entire western edge of the DEM for 30 seconds at up to 65 m^3s^{-1} and then flows downhill into a depression, which is just large enough to hold the total inflow volume. As the water accelerates down the slope a portion of the volume should overtop a bump 200 m in from the western edge and flow into a second depression. Diffusive models, like LISFLOOD-ATS are not expected to overtop the bump due to lack of an inertial term, meaning all the water should pond in the first depression. LISFLOOD-Roe is expected to simulate flow over the bump, while LISFLOOD-ACC will be unstable at the low friction value required by the test.

The depth after 300 seconds of simulation by LISFLOOD-Roe is plotted in Fig.1 and indicates the presence of water in both depressions, as expected from a full shallow water model. Time series results from the LISFLOOD-FP models and industry shallow water models at control points 1&2 on Fig. 1 are plotted in Fig. 2. In the case of LISFLOOD-ACC a higher Manning's *n* of 0.03 was used as the model is unstable at the 0.01 required by this test case because the friction is used to stabilise the scheme (see Bates et al., 2010 for a complete explanation).

The diffusive type model LISFLOOD-ATS behaved as expected, with no water overtopping the bump due to the absence of inertia in the model, meaning the depression simply fills from the bottom as water flows down the slope from the western edge. Mass errors were small (1.02×10^{-12} m^3 from an inflow of 1310 m^3) and the arrival time of the flood edge at CP1 was within two seconds of LISFLOOD-Roe. LISFLOOD-ATS velocity at CP1 initially rises at the same time as the shallow water models but then peaks early around 25% below the magnitude of the shallow water model before decreasing rapidly as the depression fills and the water surface at CP1 levels out. LISFLOOD-Roe and LISFLOOD-ACC both overtopped the bump, although a positive mass error in LISFLOOD-ACC of 25.5 m^3, compared to 0.025 m^3 in LISFLOOD-Roe meant it predicted higher water levels than LISFLOOD-Roe at both control points. This indicates that although LISFLOOD-ACC simulated water moving over the bump, the model was not stable throughout this test case, leading to a positive mass balance error during the early part of the simulation as water accelerated down slope from the inflow. The arrival time of the wetting front was later in LISFLOOD-ACC due to the higher Manning's coefficient used, although the peak velocities and final depths were within the range simulated by the industry codes. LISFLOOD-Roe provided a smoother simulation of depth and velocity transitions than LISFLOOD-ACC and some of the industry shallow water models. The EA study (Néelz and Pender, 2010) suggests that models with shock capturing capabilities provide less oscillatory solutions and the LISFLOOD-Roe results support this conclusion. Different approaches to re-sampling the two metre resolution DEM to five metres account for the 25% difference in the final depths at CP2 between the shallow water models (ISIS2D is the model that simulates the same final depth as LISFLOOD-Roe), assuming that the mass errors in these models are not significantly greater than LISFLOOD-Roe. Nevertheless, LISFLOOD-Roe filled CP2 at a slower rate than the industry codes. The reason for this can be explained based on the difference between LISFLOOD-Roe and its closest industry equivalent InfoWorks2D. InfoWorks2D uses a semi-implicit or a dual time-stepping Runge-Kutta scheme whereas LISFLOOD-Roe is first-order in time and space, which adds numerical diffusion and means smoother peaks and slower propagation times as seen in this test. All the other industrial schemes for the complete shallow water equations are second order in either space or time or both.

3.2 Rate of flood propagation over extended floodplains

This test case comprises a flat, initially dry floodplain and a point source on the centre west edge of the domain. It is designed to test the ability of the model to simulate symmetrical flooding over an extended floodplain and was test 4 in the EA benchmarking study. All three LISFLOOD-FP codes are expected to simulate the level dynamics for this test. However, the EA study results found that simpler models were unable to simulate velocity. The simplicity of the topography means the industrial codes can be compared to the LISFLOOD-FP simulations with relative confidence, although the implementation of the inflow in the industry codes might differ from the cell centred varying head method used by LISFLOOD-FP. The test case comprises of a 1000 by 2000 m floodplain at 5 m resolution, a Manning's roughness coefficient of 0.05 and uses the 5 hour inflow hydrograph shown in Fig. 3 at a 20 m wide source on the centre west edge of the domain.

The top row of Fig. 4 plots a snapshot of simulated depths from the LISFLOOD-FP models and the six commercial codes three hours into the simulation, shortly before the shoreline reached the eastern closed boundary of the domain. This allowed the greatest time period for differences between the models to emerge. All the shallow water codes, including LISFLOOD-Roe, have semi-circular shorelines with no discernable preferential flow in any direction. The flood extents simulated by LISFLOOD-ACC were greater in the diagonal indicating a preferential flow in these directions. LISFLOOD-ATS simulated similar but less pronounced preferential flow in the diagonal. Of the commercial diffusive type codes, JFLOW-GPU which is coupled in x and y, simulated a semi-circular shoreline with a slight preference for flow perpendicular to the grid, whilst FlowRoute (which is decoupled) simulates a remarkably similar preferential flow to LISFLOOD-ACC, despite using the uniform flow formula implemented by LISFLOOD-ATS. A number of tests were conducted to attempt to recreate the greater diagonal flow simulated by FlowRoute and LISFLOOD-ACC with LISFLOOD-ATS, including changing the wetting and drying parameters and friction. However, using the fixed time-step of FlowRoute and removing the linearization of the LISFLOOD-ATS scheme for shallow water surface gradients (necessary to prevent the solution stalling in the adaptive time-stepping version) lead to the increased preferential flow in the diagonal seen in FlowRoute and LISFLOOD-ACC. These changes to the numerical scheme effectively return LISFLOOD-ATS to the version developed by Bates and De Roo (2000), which was subsequently upgraded by Hunter et al. (2005) to the version used throughout this paper.

Below the snapshots of simulated depth in Fig. 4 is a matrix plotting the differences between each of the simulations at this time. All the shallow water models differ from each other at the flood edge, presumably due to the wetting algorithm adopted. Away from the flood edge they are more alike with differences <0.005 m rising up to 0.05 m within a few cells of the inflow. LISFLOOD-Roe was most like InfoWorks2D, which was not unexpected given that they both use Roe's approximate Riemann solver. Unlike all the other models, InfoWorks2D used an unstructured grid, indicating the choice of spatial discretisation had less effect on the outcome of this test case than the choice of numerical scheme, as would be expected over flat topography. JFLOW-GPU behaved in an almost opposite manner to LISFLOOD-ATS, with flow underestimated in the diagonal relative to the shallow water models. This led to greater depths (up to 0.025 m) 40 m diagonally from the source and lesser depths (up to 0.01 m) towards the flood edge in the diagonal. Although the LISFLOOD-ATS extents are similar to the shallow water models depths were also up to 0.01 m greater perpendicular to the inflow point. Perhaps the key point here is that all these differences are small relative to typical vertical errors in survey data and the accuracy required for strategic flood risk assessment.

Fig. 5 plots time series of depth and velocity at the four control points marked on the TUFLOW depth results in Fig. 4. To minimise confusion on the plots, simulations by the industry shallow water codes have been lumped into a single category, the interested reader is referred to the EA benchmarking study for a more detailed breakdown of these model results (Néelz and Pender, 2010). The industry shallow water codes and LISFLOOD-FP models simulated floodplain wetting to within 6 minutes of each other at the five points on the horizontal (CP1-4 or 1,3,5,6 in the EA study). On the diagonal (CP3 or 5 in the EA study) all LISFLOOD-FP and a number of the industrial models wetted at 60 minutes (±3 minutes), although depth increased more rapidly over the next 20 minutes in the decoupled models. This more rapid increase in depth was reflected in the velocity simulations at this point, where velocity was 7.5% and 8.8% greater than LISFLOOD-Roe when simulated by LISFLOOD-ATS and LISFLOOD-ACC, respectively. The velocities on the horizontal were lower than LISFLOOD-Roe and the majority of the shallow water codes by a similar margin. Interestingly, LISFLOOD-ACC continued to simulate greater velocity on the diagonal for the remainder of the simulation, whilst the LISFLOOD-ATS velocities tended towards the shallow water codes then dropped below them after 175 minutes. This decrease in velocity was most noticeable in the depth simulations once the inflow hydrograph began to decrease at 250 minutes, demonstrating the effect of the LISFLOOD-ATS linearization at low slope (see Table 2). This is intuitively sensible since the inflow is driving the head change at the source and the water surface slope across the domain, which when shallow will initiate the linearization. A fixed time-step formulation or formulation without the linearization would appear appealing on this basis, however as the water surface slope decreases towards zero the necessary time-step to avoid instability (checker boarding) will become infinitesimally small and computationally impractical.

Overall depths simulated by all the models were within 10% of each other, while inundation arrival times at CP 4 were spread over a <3 minute window after 60 minutes of simulation. In this test case it is not possible to pick out depth differences between the codes that can be attributed to the physical representation of the flow given the sensitivity to decoupling, linearization at low gradient, wetting method and the dominance of diffusion. At CP's 1-3 differences in peak velocity between the shallow water and simpler codes decreased with distance from the source where slopes and depths were lower, although the peak differences did not exceed 10%. It is worth noting that the differences between the industry models at CP1 were greater than the differences between the LISFLOOD-FP models, but also that the maximum velocities recorded in these plots were below a gentle 0.5 ms^{-1}. The next test case of a valley flooding following a dam failure represents a higher energy and less symmetrical test case.

3.3 Valley flooding following dam failure

This test case requires the models to simulate a valley flooding flood following a dam failure. For events of this type, flow depth, velocity and arrival time are all regarded as important factors for risk and hazard assessment because potentially dangerous velocities are expected. Given the EA results, LISFLOOD-Roe and LISFLOOD-ATS were expected to simulate maximum depths that were consistent with the industry codes, but the diffusive model was not expected to simulate velocity well due to a lack of inertia. LISFLOOD-ACC has not been tested on a case like this previously. The test case uses the hydrograph in Fig. 6 evenly spread over a 210 m inflow boundary (or 4 cells at 50 m resolution), a Manning roughness coefficient of 0.04 and a closed downstream boundary. A 50 m DEM was used in test case 5 in the EA benchmarking study. Here the LISFLOOD-FP simulations were also run at the 10 m resolution of the best available DEM (Fig. 7) because significant simulation differences were observed at the higher resolution. Simulations from the industry codes are available at 50 m resolution from the EA study. However, the modellers in the EA study were asked to convert from the supplied 10 m resolution DEM to a 50 m resolution DEM and were given freedom to choose the lower left corner of the domain. This makes it difficult to perform a cell to cell overlay of the results in some cases and introduces topographic differences to the models (e.g. was the DEM re-sampled or smoothed to the 50 m resolution?). Therefore, flood extents from the industrial codes are not assessed for this test case, whilst the analysis of point time series should be interpreted with caution. This illustrates the need to implement different models in the same code in order to obtain sufficient experimental control in many benchmarking studies, especially as test cases become more complex.

Table 5 is a contingency table comparing binary inundation extents from the 50 m resolution LISFLOOD-FP models. LISFLOOD-Roe simulated a greater inundation extent than both of the simpler models, with an additional 153 (4.2% of wet/wet) and 156 (4.3% of wet/wet) cells inundated compared to LISFLOOD-ACC and LISFLOOD-ATS, respectively. The simpler models were more alike, with LISFLOOD-ACC simulating 3 (0.1% of wet/wet) additionally wet cells compared to LISFLOOD-ATS. The maximum flood depths simulated by the LISFLOOD-FP models are plotted on the top row of Fig. 8(i, ii, iii), with the differences between models below (iv, v, vi). At this resolution LISFLOOD-Roe was clearly affected by instability at the flood edge where it simulated depths up to 0.6 m greater than the simpler models, which also accounts for most of the additional cells inundated by this model. Note however, that the increased depths at the flood edge were short lived and that the mass balance errors in the model are below 0.1% of the water volume. Nevertheless, the mass errors for LISFLOOD-Roe ($-8x10^{3}$ Table 4) were significantly higher than those of LISFLOOD-ACC ($8x10^{-9}$) and LISFLOOD-ATS ($4x10^{-7}$). The mass errors from the simpler models are essentially a reflection of numerical precision of the continuity equation, with the mass error from LISFLOOD-ATS being greater because it need 194 times as many time-steps as LISFLOOD-ACC.

Water surface elevation dynamics were recorded at the six control points in Fig. 7. These points were also used by the industrial codes in the EA benchmarking study. Fig. 9 plots simulated water surface elevation over time, whist Fig. 10 plots the corresponding velocity. LISFLOOD-Roe simulated a later arrival time of the wetting front and a slower increase in water depth than the industrial codes. Although the slower increase in depth was also seen at CP2 in the flow over a bump test case, the differences to the shallow water models were larger as the travel distance is larger too. LISFLOOD-Roe had difficulty simulating the wet/dry edges at this resolution despite reducing the α coefficient in the time-step equation (Table 1) to 0.3 for this case. Furthermore, the way inflow to the domain is handled (simply changing head in the inflow cell) may not being adequate in this case.

Despite the timing issues, peak velocities for all LISFLOOD-FP models were always within the range simulated by the industry codes, while peak levels were within the range at CP's 1,3,4&6 and <10% lower at CP's 2&5. LISFLOOD-ATS and ACC simulated lower water surface elevations than the industrial codes at 50 m resolution, except at the bottom of the reach where water ponds due to the closed downstream boundary. Although arrival times were within 15 minutes of the shallow water models, the rate of rise in water surface elevation was consistently quicker (as seen in the previous test case) and the discrepancy between the models increased with distance downstream, this could potentially indicate greater numerical diffusion in the model which simulated smoother depth increases. As mass balance errors were insignificant, the higher rate of water level rise tended to result in greater peak velocities. Peak velocities for LISFLOOD-ACC and –ATS were within the shallow water model estimates at CP 5, <10% greater at CP's 1&4 and <20% greater at CP's 1, 2&6 at 50 m resolution. For this test case, the EA benchmarking study found that the diffusive type models produced oscillatory estimates of velocity (not shown here) that were sometimes over 100% different from the shallow water model simulations at points 4 and 5. However, this was not the case with the LISFLOOD-ATS because velocity simulations were within 20% of the shallow water models. Therefore, the industry diffusive models failed this test due to some unreported aspect of their implementation rather than the lack of flow process representation in the diffusive type model.

Velocity and water surface elevation data were recorded at 1 minute intervals by the industry models, so the same convention was adopted here. To evaluate the sensitivity to how frequently results were recorded the sampling rate was increased to 5 seconds. This increased water surface elevation by at most 0.003 m at CP3 but had a greater effect on velocity with peak values increasing by up to 0.189 ms^{-1} (8.9%) at CP1 and CP3. This temporal resolution effect is significant when comparing peak velocities from the models at these two control points because it is of similar magnitude to the differences between models.

The differences in water surface elevations at the beginning of the simulation reflect the differences in DEM elevation between the models (e.g. dry bed) that result from allowing the modeller to decide how to convert from a 10 m to 50 m resolution DEM. These bed elevation differences were sometimes over 50% of the differences between the model simulations (See CP 4 in particular). Therefore, before examining the 10 m results in detail, a quick test was implemented to estimate the magnitude of the resolution effect on model simulations relative to the differences between model formulations at 50 m resolution. For this experiment the 10 m resolution DEM was re-sampled to 20, 40, 50, 60, 80 & 100 m resolutions using a nearest neighbour approach. These DEM's were then used for simulation by the LISFLOOD-ACC model, as this was the most scalable model formulation in terms of computation time and model stability. Fig. 11 plots the effect of model and DEM resolution change on peak water surface elevations and velocities as well as the timings of velocity peaks. Each block of bars is one of six control points from Fig. 7, with the individual bars in each block representing the different DEM resolutions from 10 m (left) to 100 m (right). The affect of resolution on maximum water surface elevation (Fig. 11a) was up to 20 cm or 5% of the depth, with the greatest difference at control point 5. For velocities the affect of resolution was up to 0.612 m^3s^{-1} or 20% of the velocity at control point 3 (Fig. 11c). The changes in velocity with resolution have both a random component due to alterations in flow pathways with resolution and a systematic decrease in wave speed with courser resolution, which is better represented by the up to 25 minute changes in peak velocity arrival times (Fig. 11d). This is a rather simple exploration of the model sensitivity to DEM resolution and does not separate any scalability issues with the model formulation from affects of changing topography, while assuming the 10 m DEM is error free. However, the various treatments of the DEM in this paper and by the industry models demonstrate that for this test case the resolution and sampling of the topography had a similar or greater magnitude effect on model simulations than model formulation, highlighting the importance of floodplain topography, as demonstrated by numerous studies (Fewtrell, 2008; Yu and Lane, 2006; Sanders 2007; Wilson and Atkinson 2007). Therefore, although the diffusive type models were less able to simulate the hydraulics over the transitions in slope seen on this reach, the simulations of hazard were similar given the sensitivity to factors such as sampling intervals and DEM treatment.

For the 10 m resolution test the relative behaviour of the three models changed. LISFLOOD-Roe and LISFLOOD-ACC simulations of depth and velocity were more alike than LISFLOOD-ACC and ATS (see plots of maximum depths in Fig. 8 and time series data in Fig. 9&10), with both converging towards the results obtained from the 50 m resolution industry shallow water models. At 50 m resolution differences between the LISFLOOD-ACC and LISFLOOD-ATS simulations of maximum depth were an order of magnitude smaller than the differences between these simpler models and LISFLOOD-Roe, with differences <0.01 m in the area where water ponds at the bottom of the reach (northeast corner). However, at 10 m resolution LISFLOOD-ATS under predicted the depths from the other two models, with a difference in maximum water surface elevation of <0.03 m, while also simulating depths and velocities within a few percent of the 50 m resolution simulation from this model. Therefore, the increase in resolution to 10 m has caused the LISFLOOD-ACC model to behave more like a full shallow water model, whereas at 50 m resolution it behaved in a similar manner to the diffusive model. The LISFLOOD-Roe 10m simulations fall within the range of levels and velocities simulated by the 50 m resolution industry models, while the mass errors (Table 4) have decreased. Furthermore, the maximum depth plots in Fig. 12 show no evidence of the instability at wet/dry edges seen at 50 m resolution.

At 10 m resolution the greatest differences between the LISFLOOD-Roe and LISFLOOD-ACC models occurred in areas of deep water at the base of steep slopes. Typically, the difference between the models are <0.3 m, however LISFLOOD-ACC over predicted LISFLOOD-Roe by up to 1.6 m for a roughly 500 m by 500 m region of deep water at the bottom of a slope close to the dam breach. This is a region where we find transitions from supercritical to subcritical flow so it is very unlikely to be simulated well by LISFLOOD-ACC. However, it is interesting that these locally large errors have not propagated down the valley, where the levels, velocities and timings are within the range simulated by the industry shallow water models. This is consistent with the finding of Hunter *et al*. (2005) that local hydraulic shocks do not necessarily impact on wave propagation and that where these do not dominate a test case or results in large mass balance errors it may still be possible to use a simplified model.

The differences between the models are further illustrated by the long section plots of bed elevation and maximum depth for the top 10,000 m of the reach in Fig. 12. Plot (a) on this figure shows the maximum water surface elevations for the three LISFLOOD-FP model simulations at 10 m resolution. As stated previously, the models are most alike on the steeper sections of the domain except at 1,500 to 2,000 m where LISFLOOD-ACC over-predicted the other models. In areas of shallow gradient LISFLOOD-ATS under-predicted the other two models as noted in Fig. 8(xi & xii). Also plotted on this long section are the maximum velocity (c) and depth at the time of maximum velocity (b) from LISFLOOD-Roe. This was done to demonstrate that maximum depth was not coincident with maximum velocity on shallower sections of the model domain and also that LISFLOOD-Roe maximum velocities could sometimes occur during cell wetting due to the use of a momentum threshold that required a depth of flow between cells of 0.01 m before the flow equation was implemented (See Table 2). The implication for hazard estimation where the hazard is a product of both depth and velocity is that maximum simulated depth and velocity may only be appropriate for hazard estimation on the steeper sections of the domain, but are likely to overestimate hazard on sections with lower gradients. Calculating hazard at each time-step through a simulation and taking the maximum will be necessary in these locations and the method adopted for this is more significant in terms of resulting hazard than the choice of model for this test.

3.4 Dam break

This test case (EA test 6B) is designed to evaluate the code's ability to simulate hydraulic jumps and wake zones behind buildings and is a 20x scaled up version of the flume study by Soares-Frazao and Zech (2002). Only LISFLOOD-Roe is expected to give satisfactory simulations for this test due to the dominance of supercritical flow in this test case and lack of shock capturing capability in the other LISFLOOD-FP models. The domain comprises an 8 m deep, 135 m by 72 m reservoir that flows through a 20 m wide gate into a 72 m wide flume with a single building 68 m from the gate. The flume has an initial water depth of 0.4 m and a total length of 2020 m. Simulations were run for 300 seconds from initially still water conditions with a Manning's coefficient of 0.05.

To illustrate the test case results, inundation depths simulated by LISFLOOD-Roe are plotted at 5 second intervals for the first 30 seconds of the simulation in Fig. 13. The model performed as expected, with a hydraulic jump developing in front of the building from 15 seconds onwards and a wake zone behind the building from 20 seconds onwards. To compare the LISFLOOD-FP models and industry shallow water codes water level time-series were recorded at the six control points in Fig. 14, although neither LISFLOOD-ATS or LISFLOOD-ACC were expected to simulate this test case adequately as they lack the necessary physics. LISFLOOD-ATS provided a smooth but inaccurate solution to the test without simulating the hydraulic jump, although the mass conservation was the best of the three models. LISFLOOD-ACC was the least accurate of the LISFLOOD-FP models and had a 30% volume error because some flows between cells were sufficiently high to cause negative cell water depths when the continuity equation was implemented. This confirms, as expected, the unsuitability for this scheme for this test and situations where a significant proportion of the flow will be supercritical at times and in areas of interest. It is not clear from these results if this model failed primarily due to the lack of advection terms and/or because of the numerical solver used. However, advection will be necessary when velocities vary rapidly in time (e.g. transitional flows), while the results from the industry schemes and other LISFLOOD-FP models demonstrate, as expected, that a shock capturing shallow water model is necessary for these conditions.

Overall LISFLOOD-Roe provided a similar solution to the industry shallow water models. The simulated depth and velocity dynamics were smoother than the codes without shock capturing capabilities and most like those of InfoWorks2D, indicating the importance of the choice of shallow water solver in this test as discussed by Néelz and Pender (2010). This test has demonstrated that both simpler LISFLOOD-FP models should be avoided in situations where hydraulic jumps are expected to affect flood wave propagation.

4 Discussion

This paper has applied three versions of the LISFLOOD-FP model with different process representations to four test cases that were used for benchmarking industry standard two-dimensional model codes. Differences between the LISFLOOD-FP models were evaluated using a set of controlled tests that would have been difficult to implement without a universal code environment to manage the model state variables and parameters. This discussion will be structured in two parts, with the first part dealing with the results from the three models from each test and the degree of physical complexity needed to simulate inundation under versions scenarios, followed by a second section on the implication of these results on benchmarking best practice.

4.1 How much physical complexity is required?

For the test cases where flows were subcritical and varied gradually in time simulations of velocity, depth and inundation extent from the three models and the industry codes were broadly consistent with differences between models due to physical complexity often obscured by more subtle issues. The simulations of flood propagation over an extended floodplain provide an example of this problem for depth simulation because of the sensitivity to decoupling, linearization of the diffusive model at low slopes and to a lesser extent wetting and drying parameters. Despite these factors, depths simulated by industry shallow water and the three LISFLOOD-FP models were within 10% of each other for this test, while inundation arrival times were spread over a <6 minute, but often <3 minute, window after up to 60 minutes of simulation. The velocity dynamics showed more variation between the codes, with the two simpler LISFLOOD-FP models, where the flow equations are decoupled in x and y, tending to under-predict the LISFLOOD-Roe velocity when aligned with the grid and over-predict on the diagonal, except when the time-step linearization takes effect in LISFLOOD-ATS. Although this is a limitation, being unable to simulate symmetry was not an obvious problem in the real world test cases and given the results from JFLOW GPU not a problem that relates to physical complexity. Nevertheless, if symmetry is essential then decoupled schemes should be avoided. An ability to simulate symmetry may thus be a theoretically interesting property for a hydraulic model, but one which may not have great practical relevance.

For the valley flooding following dam failure at 50 m resolution, maximum simulated depths were lower in LISFLOOD-ATS and -ACC, although the sensitivity to subtle choices over how to sample the topography from the 10 m DEM and the grid resolution of the model were as important in determining local variations in depth and velocity. LISFLOOD-Roe simulated later arrival times and slower increases in water levels than the other industry shallow water models at 50 m resolution, indicating the model had too much numerical diffusion at this scale, while being unable to simulate the wet/dry edges in a satisfactory manner. At 10 m resolution simulations from LISFLOOD-ACC and LISFLOOD-Roe were within the range of industry codes. Further work to improve the scalability of the codes, particularly LISFLOOD-Roe, when applied to this test is needed. For LISFLOOD-ATS the absence of inertia was evident around the regular transitions in slope along the reach. In percentage terms, the consistency in velocity simulation was similar to the consistency in simulation of depth, although velocity was more sensitive to local DEM changes than depth which made this variable difficult to compare with the industry codes due to uncertainties in topographic sampling.

Simulation times varied dramatically between test cases, although the LISFLOOD-FP model with the simplest physical representation (LISFLOOD-ATS) required the longest simulation time by between one and two orders of magnitude for all tests. The simulation times of LISFLOOD-Roe were consistent with the quicker explicit industry shallow water models in Néelz and Pender (2010), but the inertial model LISFLOOD-ACC was 3.2 times faster than LISFLOOD-Roe for the flooding over an extended floodplain. The flow over an extended floodplain test provides the most rigorous comparison of simulation times here because simulated depths and inundation extents were more consistent between the models in this test than the others. The simulation times for LISFLOOD-ATS are likely to seriously limit its suitability for large area, fine resolution or Monte Carlo type studies, even when the simulations are considered to be accurate enough for the task. Although not reported here all the models were tested with inappropriately long time-steps and found to be inaccurate, particularly in terms of timings and velocities meaning this should be avoided. This is especially relevant in the case of LISFLOOD-ATS where a similar time-step to that used in the models with inertia will lead to inaccurate simulation. The high computational cost of LISFLOOD-ATS means it is tempting to use an adaptive time-step similar to the shallow water models, whilst implementing a flow limiter to prevent the solution from oscillating. Hunter et al. (2005) provide a description of this approach, however the flow limiter should be avoided because it leads to a significant deterioration in the quality of simulated wave propagation.

At this point it is useful to discuss the explicit diffusive model results within the historical context of their use. These models were critical in highlighting the advantages of 2D modelling of floodplain flows over 1D approaches (Horritt and Bates, 2002), while bringing flood simulation to a wider audience by being relatively easy to code, understand and visualise. Furthermore, the results here and elsewhere (e.g. Yu and Lane, 2006; Tayefi et al., 2007; Hunter et al., 2008; Neal et al., 2009a) indicate that the inundation extents and depths typical of previous mapping work with these models would not change markedly if they were re-calculated using a more complex methodology, at least for sites where flows vary gradually and model time-steps were appropriate. Explicit diffusive model also benefit from being simple, however any perception from previous work that this simplicity leads to relative computational efficiency should be rejected in almost all cases. Thus, in an operational context the approaches available for inundation simulation have moved on from the LISFLOOD-ATS type formulation.

The flow over a bump and dam break test cases require the simulation of conditions that were expected to challenge the two simpler LISFLOOD-FP formulations. Only LISFLOOD-Roe was able to simulate the flow over the bump test case correctly. LISFLOOD-ACC could also simulate water overtopping the bump but only by increasing the roughness, while LISFLOOD-ATS did not overtop the bump as would be expected for a model which lacks inertia. Thus the diffusive and shallow water model results were consistent with the EA study, while the LISFLOOD-ACC results indicate that this model may be suitable for similar test cases where flows are subcritical and friction is greater than n=0.03. Developments to this scheme for urban applications should focus on methods to maintain stability at low friction without compromising on speed, or the development of hybrid models where the numerical scheme adapts to the flow conditions.

LISFLOOD-Roe simulated similar dynamics to the other shock capturing shallow water codes for the dam break test case. LISFLOOD-ATS and LISFLOOD-ACC were unable to simulate the hydraulic jump as expected and should not be used if such features are essential to the simulation, i.e. where the influence of the shocks extends away from their local vicinity and affects wave propagation globally in the model. Where this occurs appears easy to identify for LISFLOOD-ACC as in every such case examined here the mass balance errors from the model become unacceptably large (see Table 3). Hence when applying the LISFLOOD-ACC model to test cases where it was unable to emulate the full shallow water models depths and velocities to within ~10%, its mass balance error increased by many orders of magnitude. If we conclude that the model is applicable to a smaller range of scenarios than the full shallow water models, then mass balance would appear to be a good proxy for determining appropriateness and should thus always be reported. Furthermore, although LISFLOOD-ATS was unable to simulate key aspects of the flow over a bump and the dam break the model remained stable and conserved mass for all the tests undertaken here unlike the other two models.

4.2 Implications for inundation model benchmarking

The previous discussion on model complexity highlights the difficulty of benchmarking complex models, where aspects of model setup that might usually be considered as minor can obscure the headline differences between models such as the type of solver used or physical complexity. Benchmarking is undoubtedly made easier by models that share common sub-routines and input data, such as the three used here, but as this is not a practical solution for industry models. The tests conducted in the EA study established the magnitude of differences between models given a number of test cases, which allowed model responses to be classified and approaches that simulated non-behavioural dynamics to be identified. In terms of model suitability for various applications, the finding here support those of the EA model benchmarking study (Néelz and Pender, 2010), except that the performance of LISFLOOD-ATS for velocity simulation was significantly better than the industry equivalents of this code and there was no industry implementation of LISFLOOD-ACC. An important question is how significant the choice of model is in relation to other factors, including both controllable model setup decisions (e.g. resolution, mesh type and the frequency with which results are recorded) and model uncertainties (e.g. possible input flow data and DEM errors).

The valley filling test provides a convenient example of how simple model setup decisions can have as much impact on hazard mapping as choosing between the three LISFLOOD-FP models. Peak velocities at each control point were short-lived to the extent that increasing the rate at which velocity was recorded from 1 minute to 5 seconds increased peak velocity by up to 8.9 % at selected control points. This has significant implications for risk assessment because methods that take infrequent snapshots of model state variable may not capture maximum velocities. Furthermore, maximum velocity and depth were broadly coincident in time on the steeper sections of the domain, with maximum depth occurring some time after maximum velocity on the shallower sections. The implication of this for hazard estimation is that the product of maximum simulated depth and maximum velocity may overestimate hazard in particular locations if these are determined separately. Also, since peak velocity is short in duration, hazard will also change rapidly.

In addition to model setup issues that can be controlled, the significance of model choice in relation to the principal sources of uncertainty would be a useful addition to future benchmarking work. Here it was relative simple to demonstrate that simulations of the valley flooding event were as sensitive to the sampling of the 10 m topography to coarser resolutions as they were to model choice, and that the model had not converged on a grid-independent estimate of velocity by 10 m. However, this should go further in future benchmarking work by evaluating the choice of model given uncertainty in the elevation and inflow data typically used for the applications being tested.

5 Conclusions

Three two-dimensional hydraulic models with different physical representations have been benchmarked using four test cases. Well known factors such as topography were found to influence simulations, but a number of less obvious factors also cause differences in simulations as great or greater than physical complexity. A number of specific conclusions can be made:

1) Explicit diffusive type model required much longer simulation times than the models with inertia for the 2-50 m resolution applications considered here. This problem cannot be solved by using fixed longer time steps and a flow limiter because of the poor simulation of wave propagation with such methods.
2) Decoupled schemes were unable to simulate symmetry over flat topography, although similar effects on the irregular topographies tested here were not identifiable given other factors. The simulation of symmetry is therefore an interesting technical test but may have limited relevance to real world flows.
3) For test cases with gradually varying flows, simulations of velocity were surprisingly similar between the codes and usually as alike as depth in terms of % difference. This means that the simplified models may be appropriate for velocity simulation for a wider range of conditions than suggested by the EA study where gradually varied subcritical flows are expected.
4) For test cases where flows change gradually with time the difference between models are only as large as differences caused by other modelling choices (e.g. topography sampling, recording of results etc).
5) The diffusive model LISFLOOD-ATS was the least like the other codes in the vicinity of slope transitions for the valley flooding following a dam failure test case. The momentum conservation over a bump test case demonstrates how the diffusive model loses momentum too quickly when the DEM slope decreases.
6) LISFLOOD-Roe as a pure first-order in time and space scheme simulated later arrival times and slower increases in water levels than the other shallow water models at the 50 m

resolution version of the valley flooding test, and the CFL number had to be reduced in order to simulate the wet/dry edges in a stable manner at 10 m resolution.

7) Simple decisions over arbitrary modelling choices, such as how frequently to record velocity and assumptions about depth velocity correlations, can have greater impacts on hazard assessment than decisions over model physical complexity.
8) The simpler models were unable to simulate hydraulic jumps and wake zones, as expected.
9) Rigorous control in benchmarking studies is difficult to achieve, especially when undertaken with multiple codes and modellers.
10) LISFLOOD-Roe was required when there were subcritical to supercritical transitions in the flow that affect the wave propagation, but unless contra-indicated by large mass errors LISFLOOD-ACC was a faster alternative to a full shallow water model for gradually varied subcritical flows where domain-average friction typically exceeds n= 0.03.

LISFLOOD-Roe was applicable to the widest range of flow conditions, although it was inaccurate at the flood edge when adjacent velocity was high and grid resolution coarse. LISFLOOD-ACC was usually the quickest model, which would be particularly advantageous for real-time inundation forecasting, Monte Carlo type analysis or large model applications. However, for conditions where this code was not physically suitable (e.g. low friction, Froude number > 1) the model became unstable and mass balance errors became large. For LISFLOOD-ATS, the ease of use, simplicity, stability and small mass errors may be desirable where the model is applied to cases where it is difficult to check model results, where only diffusive process representation is required and where coarse resolution models are needed. However, the computational cost will be relatively high for typical strategic flood risk management applications.

Through a rigorous series of benchmarks tests of 2D hydraulic models this paper is able to draw conclusions on the degree of physical complexity required to model flood inundation. We show that for gradually varied flow full shallow water models may be unnecessarily complex, and simpler, cheaper schemes, such as the inertial wave formulation in LISFLOOD-ACC, can perform just as well, both in terms of velocity and depths. Moreover we show that subtle modelling decisions can often have more effect on results than selecting a more physically complex model. The results of this study therefore provide additional guidance to help 2D model users select the appropriate scheme for any given situation.

Acknowledgement

Jeffrey Neal was funded by the Flood Risk Management Research Consortium, which is supported by grant number EP/F20511/1 from the EPSRC and the DEFRA/EA joint Research Program on Flood and Coastal Defence. We would like to thank the three anonymous reviewers for their very helpful comments and suggestion, along with Jim Walker and Sylvain Néelz for arranging access to the EA 2D model benchmarking data sets.

References

Apel, H., Aronica, G. T., Kreibich, H. & Thieken, A. H. 2009. Flood risk analyses-how detailed do we need to be? Natural Hazards, 49, 79-98.

Aronica, G.T., Nasello, C., Tucciarelli, T. 1998. A 2D Multilevel Model for Flood Propagation in Flood Affected Areas. ASCE - Journal of Water Resources Planning and Management, Vol.124, 4.

Bates, P. D. & De Roo, A. P. J. 2000. A simple raster-based model for flood inundation simulation. Journal of Hydrology, 236, 54-77.

Bates, P. D., Horritt, M. S. & Fewtrell, T. J. 2010. An simple inertial formulation of the shallow water equations for efficient two dimensional flood inundation modelling. *Journal of Hydrology,* 387**,** 33-45.

Brufau, P., García-Navarro, P., and Vázquez-Cendón, M. E. 2002. “A numerical model for the flooding and drying of irregular domains.” Int. J. Numer. Methods Fluids, 39, 247–275.

Bradbrook, K. F., Lane, S. N., Waller, S. G. & Bates, P. D. 2004. Two dimensional diffusion wave modelling of flood inundation using a simplified channel representation. International Journal of River Basin Management, 2, 1-13.

Crowder, RA., Pepper, AT., Whitlow, C., Sleigh, A Wright, N. and Tomlin C. 2004. Benchmarking of hydraulic river modelling software packages. SCHO0305BIXN-E-P. Environment Agency, Bristol.

Cobby, D.M., Mason, D.C., Davenport, I.J., 2001. Image processing of airborne scanning laser altimetry data for improved river flood modelling. ISPRS Journal of Photogrammetry and Remote Sensing, 56(2): 121-138.

Fewtrell, T.J., Bates, P.D., Horritt, M., Hunter, N.M., 2008. Evaluating the effect of scale in flood inundation modelling in urban environments. Hydrological Processes, 22(26): 5107-5118.

Gouldby, B., Sayers, P., Mulet-Marti, J., Hassan, M. A. A. M. & Benwell, D., 2008. A methodology for regional-scale flood risk assessment. Proceedings of the Institution of Civil Engineers - Water Management, 161, 169-182.

Guinot, V. & Soares-Frazao, O. S. 2006. Flux and source term discretization in two-dimensional shallow water models with porosity on unstructured grids. International Journal for Numerical Methods in Fluids, 50, 309-345.

Hall, J.W., Dawson, R.J., Sayers, P.B., Rosu, C., Chatterton, J.B. & Deakin, R. 2003. A methodology for national-scale flood risk assessment. Proceedings of the Institution of Civil Engineers-Water and Maritime Engineering, 156, 235-247.

Hall, J.W., Sayers, P.B. & Dawson, R.J., 2005. National-scale assessment of current and future flood risk in England and Wales. Natural Hazards, 36, 147-164.

Hall, J.W., Manning, L.J. & Hankin R.K.S., 2011. Bayesian calibration of a flood inundation model using spatial data. Water Resources Research, 47, W05529.

Horritt M. S., 2000. Calibration of a two-dimensional finite element flood flow model using satellite radar imagery. Water Resources Research, 36, No. 11, 3279–3291.

Horritt, M.S., Bates, P.D., 2001. Predicting floodplain inundation: raster-based modelling versus the finite-element approach. Hydrological Processes, 15(5): 825-842.

Horritt, M.S., Bates, P.D., 2002. Evaluation of 1D and 2D numerical models for predicting river flood inundation. Journal of Hydrology, 268(1-4): 87-99.

Horritt, M.S., Di Baldassarre, G., Bates, P.D., Brath, A., 2007. Comparing the performance of a 2-D finite element and a 2-D finite volume model of floodplain inundation using airborne SAR imagery. Hydrological Processes, 21: 2745-2759.

Hunter, N.M., Horritt, M.S., Bates, P.D., Wilson, M.D. and Werner, M.G.F., 2005a. An adaptive time step solution for raster-based storage cell modelling of floodplain inundation. Advances in Water Resources, 28, 975-991.

Hunter, N.M., Bates, P.D., Neelz, S., Pender, G., Villanueva, I., Wright, N.G., Liang, D., Falconer, R.A., Lin, B., Waller, S., Crossley, A.J. and Mason, D.C., 2008. Benchmarking 2D hydraulic models for urban flooding. Proceedings of the Institution of Civil Engineers-Water Management, 161(1), 13-30.

Lamb, R., Crossley, A. & Waller, S., 2009. A fast 2d floodplain inundation model. Proceedings of the Institution of Civil Engineers - Water Management, 162, 363-370.

Leopardi A., Oliveri E. and Greco M., 2002. Two-dimensional modeling of floods to map risk-prone areas. ASCE Journal of Water Resources Planning and Management, 128, No. 3, 168–178.

Lhomme, J., Gutierrez-Andres, J., Weisgerber, A., Davison, M., Mulet-Marti, J., Cooper, A. And Gouldby, B., 2010. Testing a new two-dimensional flood modelling system: analytical tests and application to a flood event. Journal of Flood Risk Management 3(1): 33-51.

Liang, D., Falconer, R. A. & Lin, B. L., 2006. Comparison between tvd-maccormack and adi-type solvers of the shallow water equations. Advances in Water Resources, 29, 1833-1845.

Liang D., Lin B. and Falconer R. A., 2007. Simulation of rapidly varying flow using an efficient TVD-MacCormack scheme. International Journal for Numerical Methods in Fluids, 53(5), No. 3, 811–826.

McMillan, H. K. & Brasington, J., 2007. Reduced complexity strategies for modelling urban floodplain inundation. Geomorphology, 90, 226-243.

Mignot, E., Paquier, A. & Haider, S., 2006. Modeling floods in a dense urban area using 2d shallow water equations. Journal of Hydrology, 327, 186-199.

Neal, J., Bates, P., Fewtrell, T., Hunter, N. M., Wilson, M. & Horritt, M., 2009a. Distributed whole city water level measurements from the Carlisle 2005 urban flood event and comparison with hydraulic model simulations, Journal of Hydrology, 368, 42-55.

Neal, J. C., Fewtrell, T. J. & Trigg, M. A., 2009b. Parallelisation of storage cell flood models using openmp. Environmental Modelling and Software, 24, 872-877.

Néelz, S. & Pender, G. 2010. Benchmarking of 2D Hydraulic Modelling Packages. SC080035/SR2. Environment Agency, Bristol.

Roe, P. (1981). "Approximate Riemann Solvers, Parameter Vectors, and Difference-Schemes." Journal Of Computational Physics 43(2): 357-372.

Sanders, B. F., 2007. Evaluation of on-line dems for flood inundation modeling. Advances in Water Resources, 30, 1831-1843.

Schubert, J.E., Sanders, B.F., Smith, M.J., Wright, N.G., 2008. Unstructured mesh generation and landcover-based resistance for hydrodynamic modeling of urban flooding. Advances in Water Resources, 31(12): 1603-1621.

Soares-Frazao, S. and Zech, Y., 2002 Dam-break flow experiment: The isolated building test case. Available online at: http://www.impact-project.net/wp3_technical.htm

Stelling, G.S., Kernkamp, H.W.J. & Laguzzi, M.M., 1998. Delft Flooding System: a powerful tool for inundation assessment based upon a positive flow simulation. Hydroinformatics '98, eds. Babovic and Larsen, Balkema: Rotterdam, 449-456.

Syme, W.J., 1991. Dynamically linked two-dimensional/one-dimensional hydrodynamic modelling programfor rivers estuaries and coastal waters. MEngSc thesis, University of Queensland, Australia.

Tayefi, V., Lane, S.N., Hardy, R.J., Yu, D., 2007. A comparison of one- and two-dimensional approaches to modelling flood inundation over complex upland floodplains. Hydrological Processes, 21(23): 3190-3202.

Trigg, M.A. et al., 2009. Amazon flood wave hydraulics. Journal of Hydrology, 374(1-2): 92-105.

Villanueva, I. & Wright, N. G., 2006. Linking Riemann and storage cell models for flood prediction. Proceedings of the Institution of Civil Engineers, Journal of Water Management, 159, 27-33.

Werner, M.G.F., 2004. A comparison of flood extent modelling approaches through constraining uncertainties on gauge data. Hydrology and Earth System Sciences, 8(6): 1141-1152.

Werner, M.G.F., Hunter, N.M., Bates, P.D., 2005. Identifiability of distributed floodplain roughness values in flood extent estimation. Journal of Hydrology, 314(1-4): 139-157.

Wilson, M.D., Atkinson, P.M., 2007. The use of remotely sensed land cover to derive floodplain friction coefficients for flood inundation modelling. Hydrological Processes, 21(26): 3576-3586.

Yu, D. & Lane, S. N., 2006. Urban fluvial flood modelling using a two-dimensional diffusion-wave treatment, part 2: Development of a sub-grid-scale treatment. Hydrological Processes, 20, 1567-1583.

List of Figures

Table 1: Summary of test cases

EA test	Description	Tested here
1	Flooding a disconnected water body.	No
2	Filling of floodplain depressions.	No
3	Momentum conservation over a small (0.25m) obstruction.	Yes
4	Speed of flood propagation over an extended floodplain.	Yes
5	Valley flooding following a dam failure.	Yes + finer resolution
6a&b	Dam break. a) Flume scale, b) Field scale.	Yes, b only
7	River to floodplain linking.	No
8a&b	Urban flood. a) Rainfall, b) Rainfall and sewer surcharge.	No

Table 2: Model attributes

Model	**ATS**	**ACC**	**Roe**
Key reference	(Hunter et al., 2005)	(Bates et al., 2010)	(Villanueva and Wright, 2006)
Wave properties	Diffusive	Inertial shallow water	Full shallow water
Scheme	Finite difference (forward differences) explicit		Finite volume explicit
Mesh	Cartesian Grid with staggered *h* and *Q*		
Solver	None – Analytical		Approximate Roe Riemann solver
Time stepping	$\Delta t_{max} = \frac{\Delta x^2}{4} \frac{2n}{h_{flow}^{\frac{5}{3}}} \left\| \frac{\Delta h}{\Delta x} \right\|^{\frac{1}{2}}$	$\Delta t_{max} = \alpha \frac{\Delta x}{\sqrt{gh}}$	$\Delta t_{max} = \alpha \frac{\Delta x}{\|v\| + \sqrt{gh}}$
Mass conservation	$h_{i,j}^{t+\Delta t} = h_{i,j}^{t} + \Delta t \frac{Q_{x\,i-1,j}^{t+\Delta t} - Q_{x\,i,j}^{t+\Delta t} + Q_{y\,i,j-1}^{t+\Delta t} - Q_{y\,i,j}^{t+\Delta t}}{\Delta x^2}$		
Courant number (α)	Effectively 1.0	0.7 unless stated	
Shock capturing	No		Yes
Coupling in x and y	No - 1D across each cell edge		Yes
Linearization of scheme at low slope	$if\ \Delta h < \Delta x c$ where *c* = 0.0002	No	
Roughness	Manning's: Global or distributed (linear interpolation between cells). However, as the physics represented in the three models is different, the physical meaning of friction in the models differs.		
Pre-processing	Interpretation of test case was ensured to be identical between models because all access the same state variables.		
Topography (z)	Raster grid, depth of flow (h_{flow}) defined as the difference between the highest water free surface in the two cells and the highest bed elevation.		
Domain boundary/ Internal boundary (wall)	Zero flux if cell elevation exceeds adjacent water surface elevation		Brufau et al. (2002)
Point/boundary inflows	Head change only for these test cases.		
Wet/dry threshold	Depth threshold (0.001 m)		Depth threshold for wetting (0.001 m), additional threshold for momentum (0.01 m)
Numerical precision	All state variables and parameters are double precision.		
Executable	LISFLOOD-FP version 4.4.13 complied with the 64-bit Intel C++ compiler for Linux version 10.1.015. Static executable using O3 compiler optimisation with OpenMP parallelisation (see Neal et al., 2009).		
Hardware	Linux operating system running on two quad-core 2.8 GHz Intel Xeon processor (E5462) with 6 MB cash each and 16 GB of RAM.		

Where *x* is distance, *n* is Manning's roughness coefficient, *Q* is flow rate, *h* is water depth, h_{flow} is the depth of water through which water can flow, *g* is acceleration due to gravity, α is the Courant number, *v* is flow velocity and *c* is a typically small water depth threshold.

Table 3: Summary of test case simulation times (minutes).

	Test 3		Test 4		Test 5 – 50 m		Test 5 – 10 m		Test 6b	
	Simulation time	Number of time-steps	Simulation time	Number of time-steps	Simulation time	Number of time-steps	Simulation time	Number of time-steps	Simulation time	Number of time-steps
Roe	0.07	905	6.48	15291	2.55**	56211	302.19^{+*}	207487	4.67	18176
ACC	0.03	900	1.97	10551	0.68	21147	344.11^{+**}	260676	0.67	18001
ATS	1.52	82835	228.95	654581	161.13	4102887	6415.21^{++}	1.02×10^{8}	182.15	4819760

*cfl number reduced to 0.5 for stability

**cfl number reduced to 0.3 for stability

$^{+}$run on two CPU cores

$^{++}$run on eight CPU cores

Table 4: Summary of mass balance errors and mass balance errors as a percentage of input volume at the end of each model simulation. Note: water does not leave the domain in any of these test cases.

	Test 3	Test 4	Test 5 – 50 m	Test 5 – 10 m	Test 6b
Roe	2.50×10^{-2}	-2.00×10^{3}	-8.81×10^{3}	-7.05×10^{3}	-2.19×10^{0}
ACC	2.55×10^{1}	1.85×10^{-12}	8.01×10^{-9}	2.47×10^{4}	-3.68×10^{2}
ATS	1.02×10^{-12}	6.05×10^{-9}	4.22×10^{-7}	4.72×10^{3}	-1.42×10^{-7}
Domain Volume	1.31×10^{3}	2.85×10^{5}	9.44×10^{6}	9.44×10^{6}	1.29×10^{3}
Mass error as a percentage of domain volume					
Roe	0.002%	0.702%	0.093%	0.075%	0.170%
ACC	1.947%	<0.001%	<0.001%	0.262%	28.527%
ATS	<0.001%	<0.001%	<0.001%	0.050%	<0.001%

Table 5: Contingency tables for wet dry comparisons between LISFLOOD-FP models for 50 m resolution valley flooding test case

		LISFLOOD-Roe		LISFLOOD-ATS	
		Wet	Dry	Wet	Dry
LISFLOOD-ACC	Wet	3597	1	3595	3
	Dry	153	53624	0	53777
LISFLOOD-ATS	Wet	3594	1		
	Dry	156	53624		

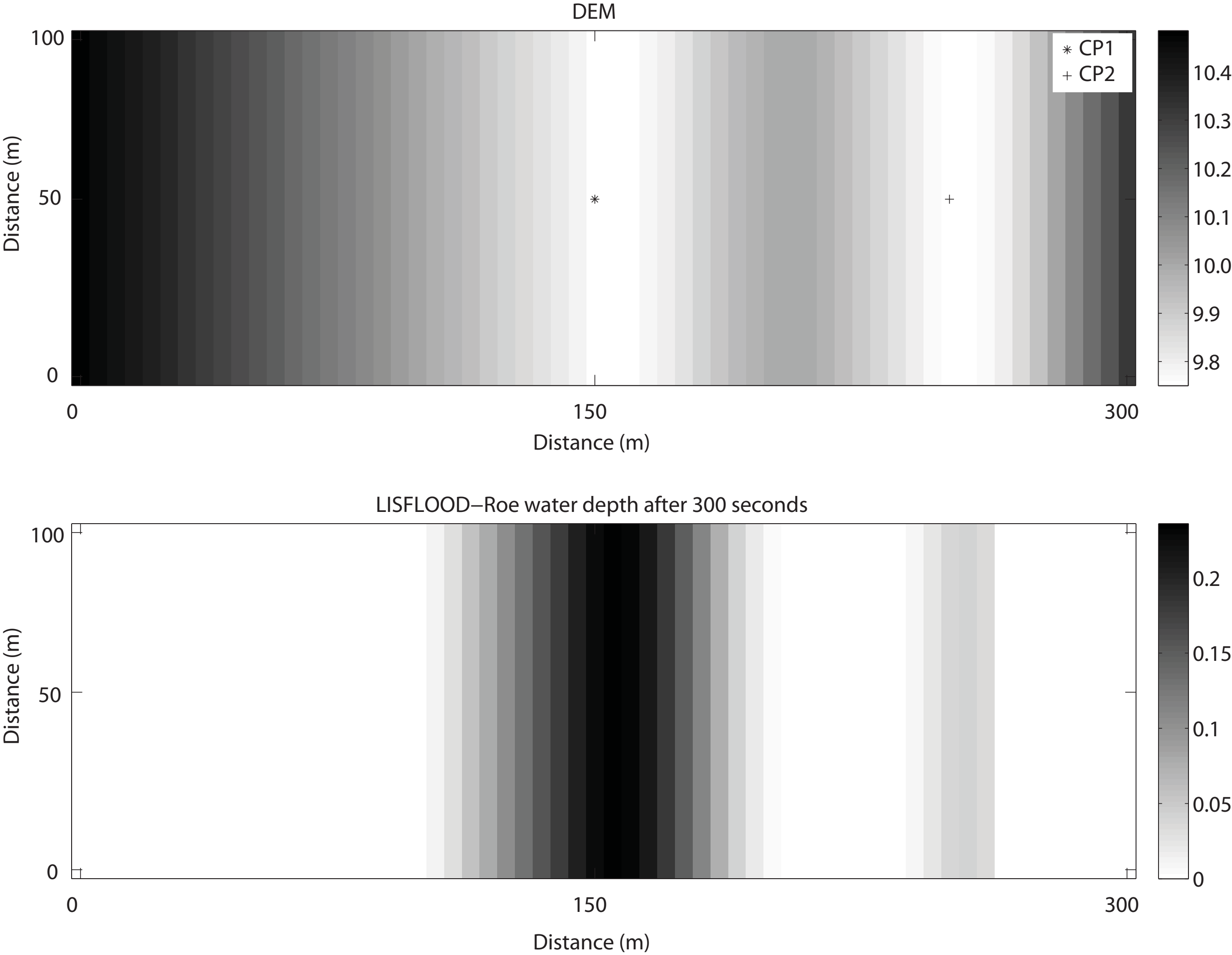
DEM
CP1
CP2
Distance (m)
100
50
0
150
300
10.4
10.3
10.2
10.1
10.0
9.9
9.8
LISFLOOD–Roe water depth after 300 seconds
0.2
0.15
0.1
0.05
0

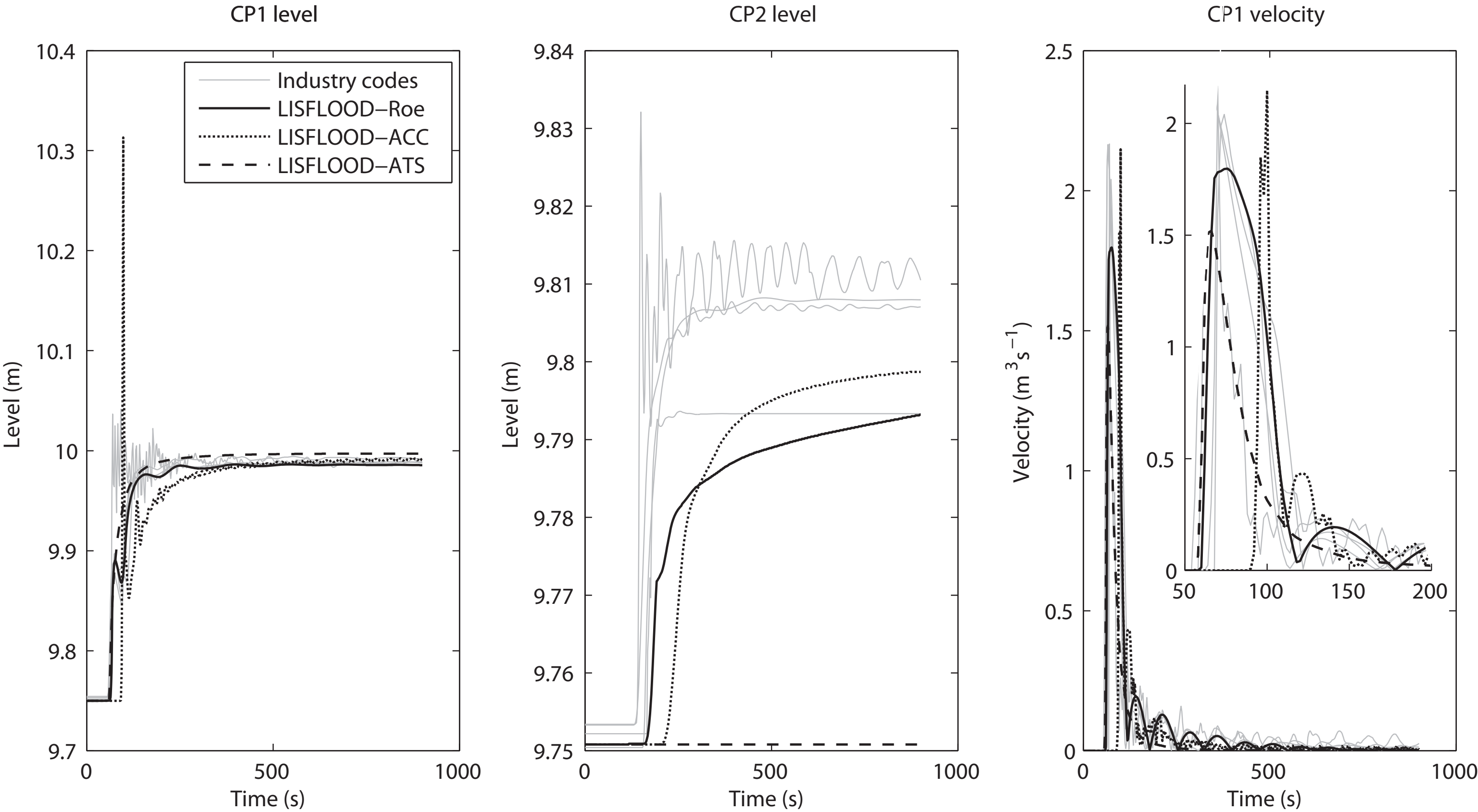
CP1 level
Industry codes
LISFLOOD–Roe
LISFLOOD–ACC
LISFLOOD–ATS
Level (m)
Time (s)
CP2 level
Level (m)
Time (s)
CP1 velocity
Velocity ($m^3 s^{-1}$)
Time (s)

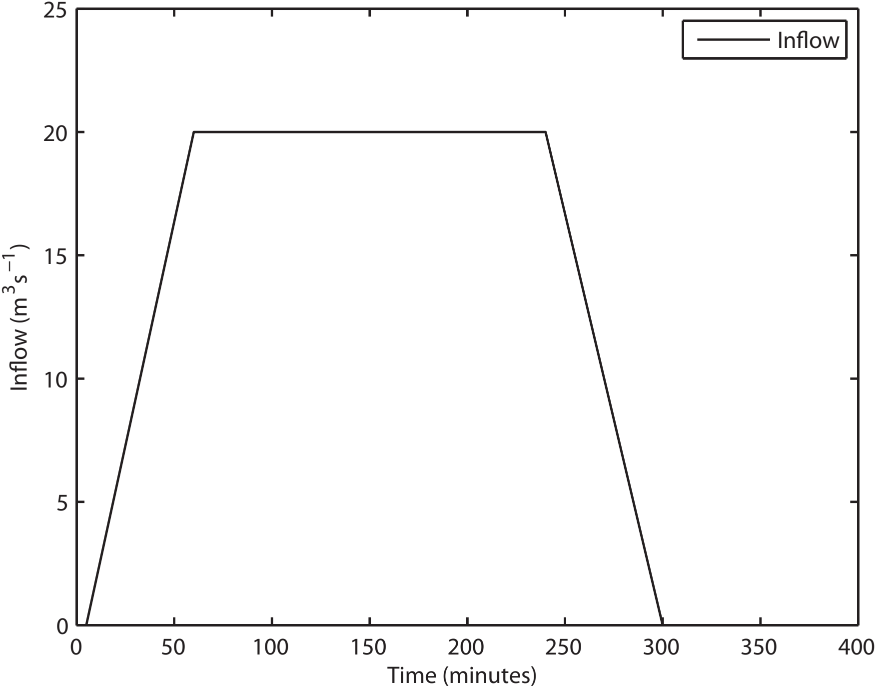

Inflow
Inflow (m^{3}s^{-1})
Time (minutes)
0
5
10
15
20
25
0
50
100
150
200
250
300
350
400

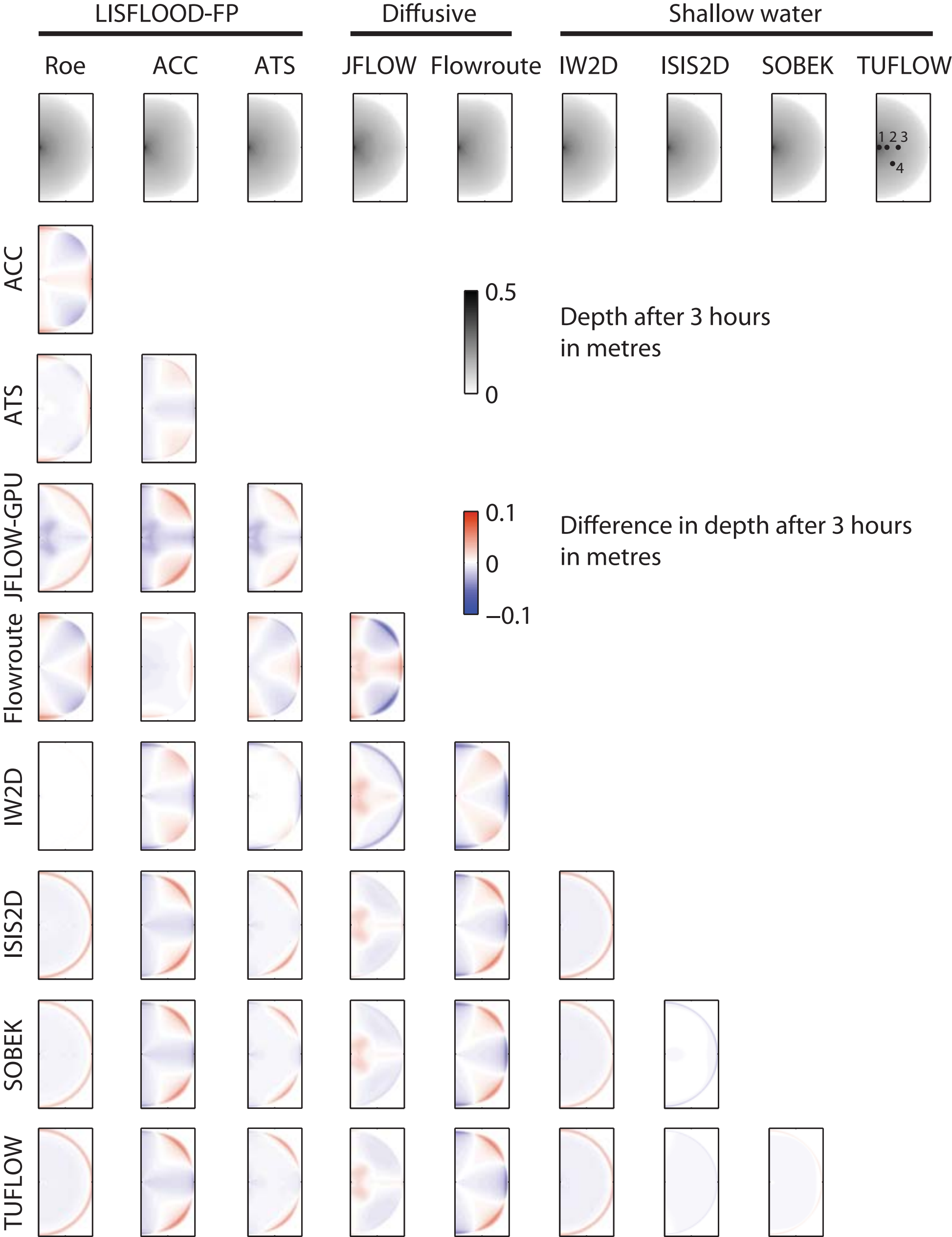
LISFLOOD-FP
Diffusive
Shallow water
Roe
ACC
ATS
JFLOW
Flowroute
IW2D
ISIS2D
SOBEK
TUFLOW
1 2 3
4
ACC
ATS
JFLOW-GPU
Flowroute
IW2D
ISIS2D
SOBEK
TUFLOW
0.5
0
Depth after 3 hours in metres
0.1
0
−0.1
Difference in depth after 3 hours in metres

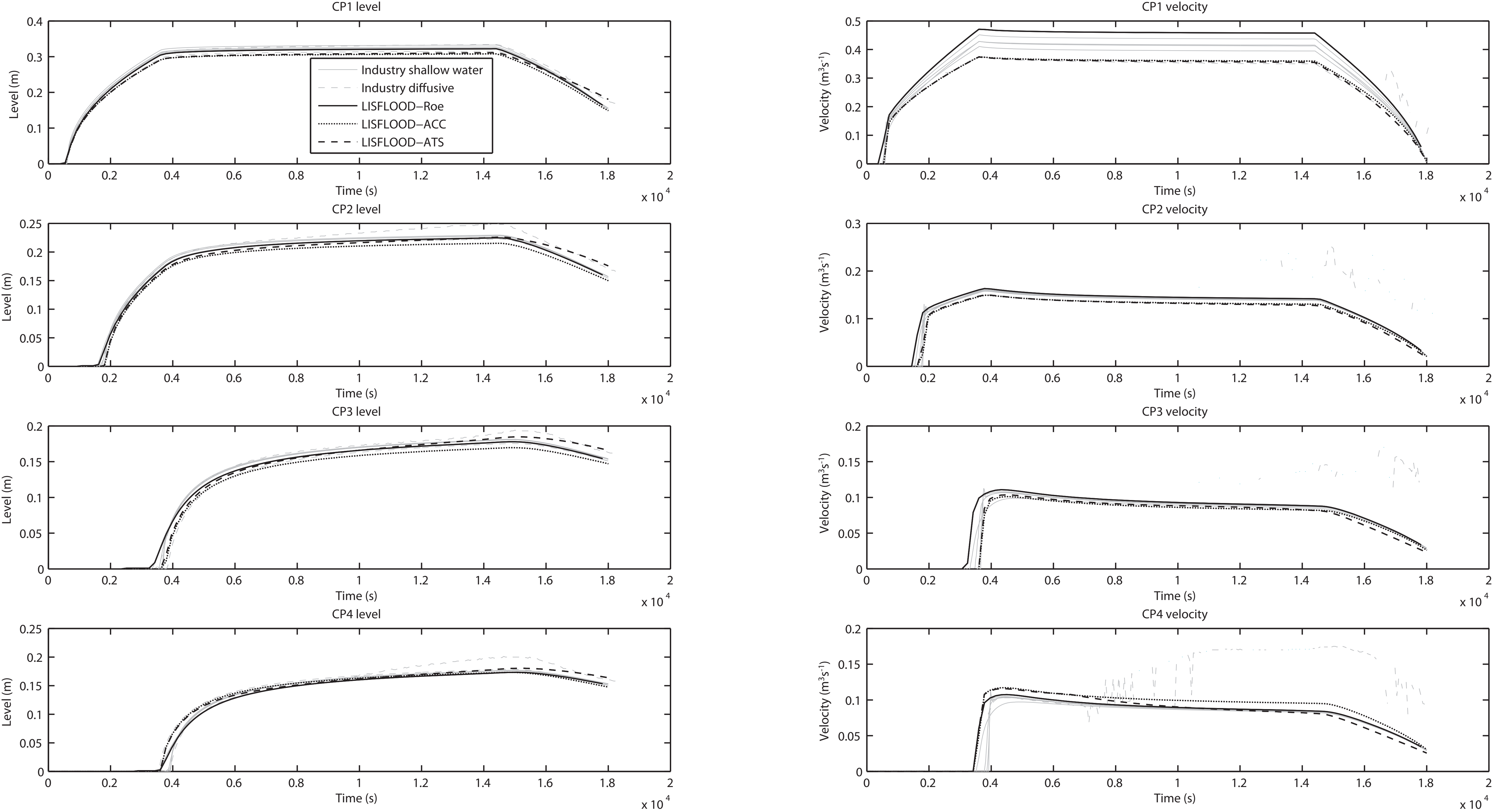
CP1 level
CP1 velocity
CP2 level
CP2 velocity
CP3 level
CP3 velocity
CP4 level
CP4 velocity
Level (m)
Velocity (m3s-1)
Time (s)
x 10^4
Industry shallow water
Industry diffusive
LISFLOOD–Roe
LISFLOOD–ACC
LISFLOOD–ATS

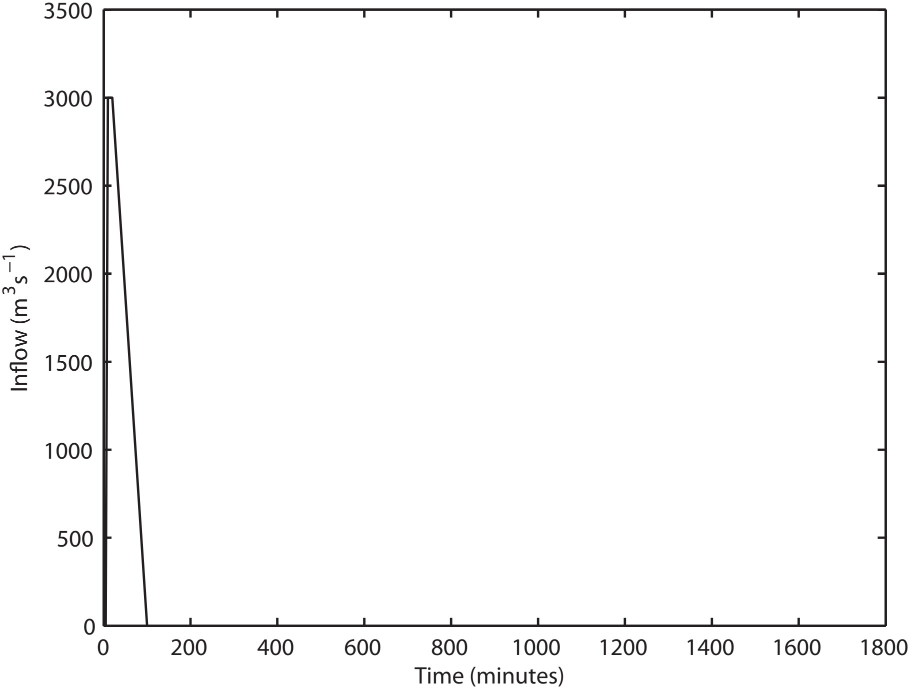

3500
3000
2500
2000
1500
1000
500
0
Inflow (m3 s−1)
0
200
400
600
800
1000
1200
1400
1600
1800
Time (minutes)

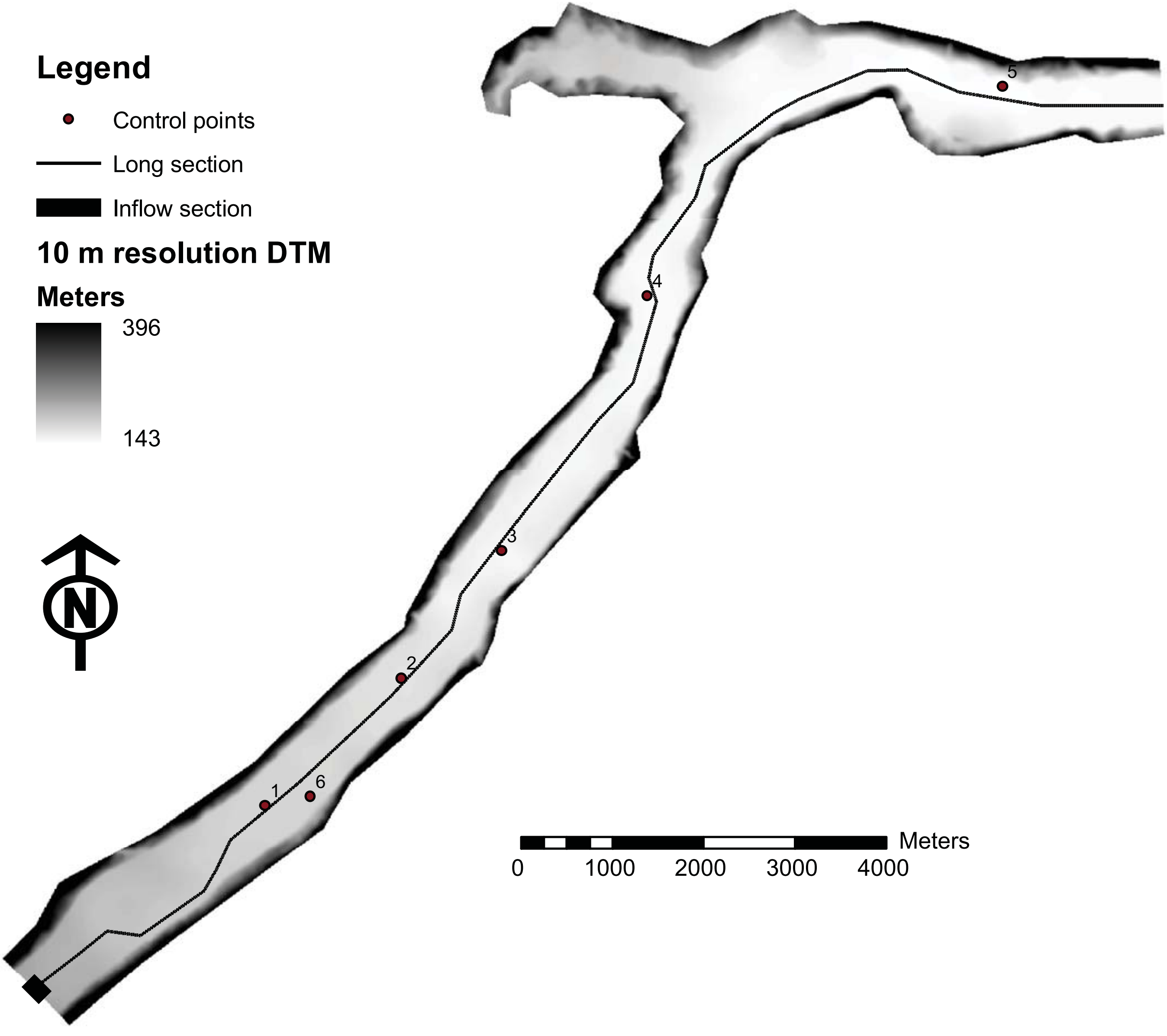

Legend
Control points
Long section
Inflow section
10 m resolution DTM
Meters
396
143
N
1
2
3
4
5
6
Meters
0
1000
2000
3000
4000

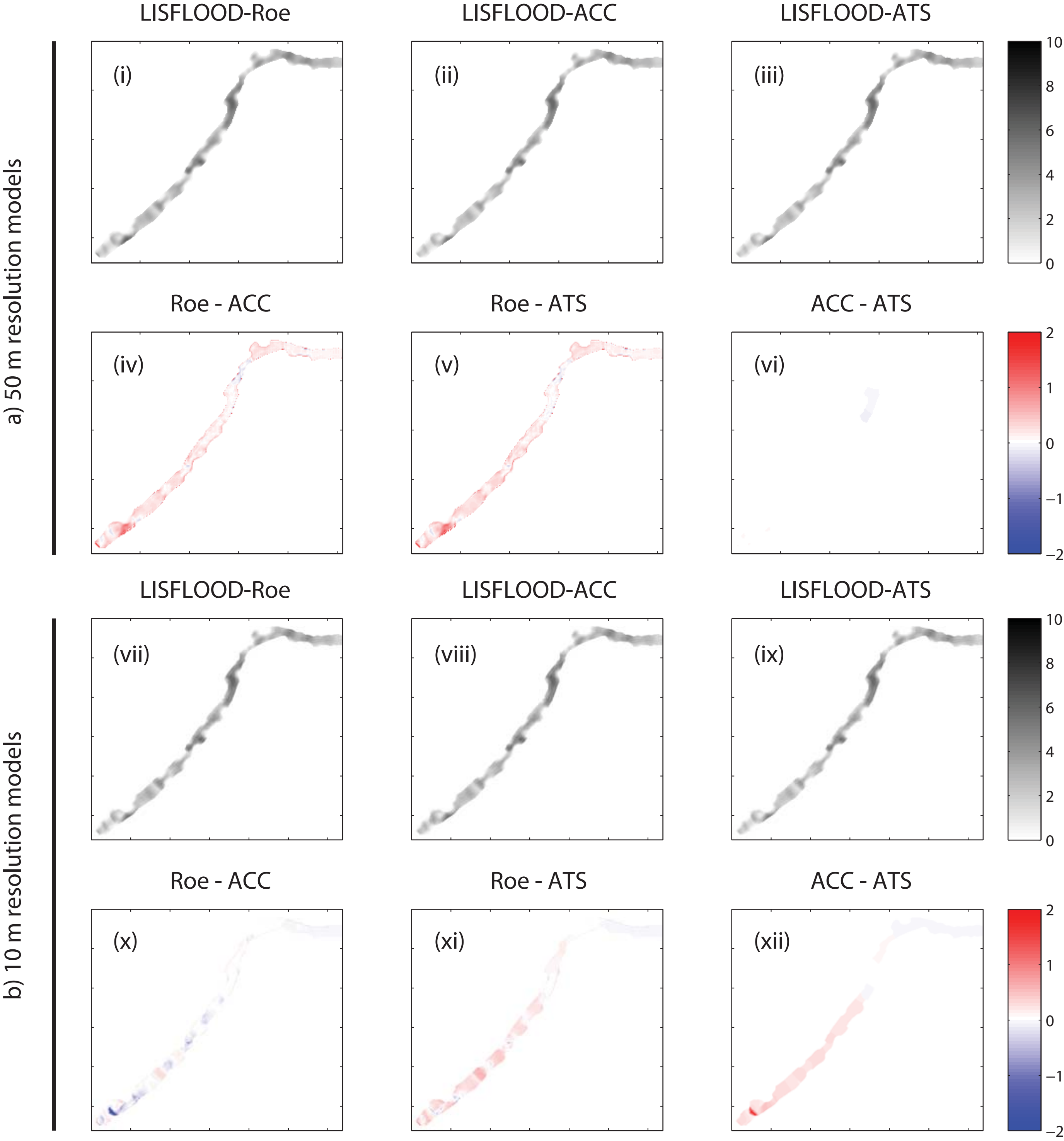
LISFLOOD-Roe
LISFLOOD-ACC
LISFLOOD-ATS
(i)
(ii)
(iii)
Roe - ACC
Roe - ATS
ACC - ATS
(iv)
(v)
(vi)
a) 50 m resolution models
LISFLOOD-Roe
LISFLOOD-ACC
LISFLOOD-ATS
(vii)
(viii)
(ix)
Roe - ACC
Roe - ATS
ACC - ATS
(x)
(xi)
(xii)
b) 10 m resolution models
10
8
6
4
2
0
2
1
0
−1
−2

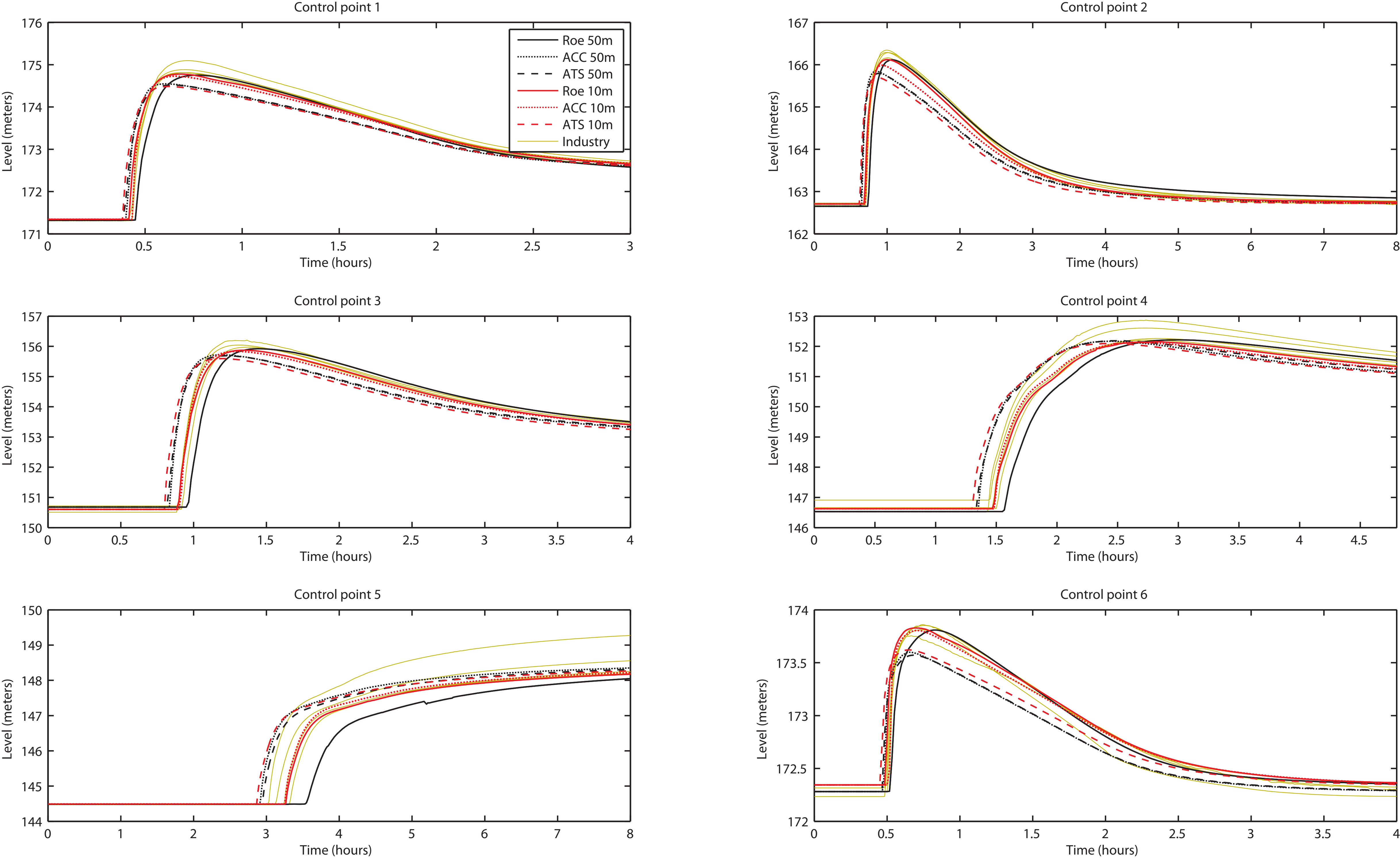

Control point 1
Control point 2
Control point 3
Control point 4
Control point 5
Control point 6
Roe 50m
ACC 50m
ATS 50m
Roe 10m
ACC 10m
ATS 10m
Industry
Level (meters)
Time (hours)

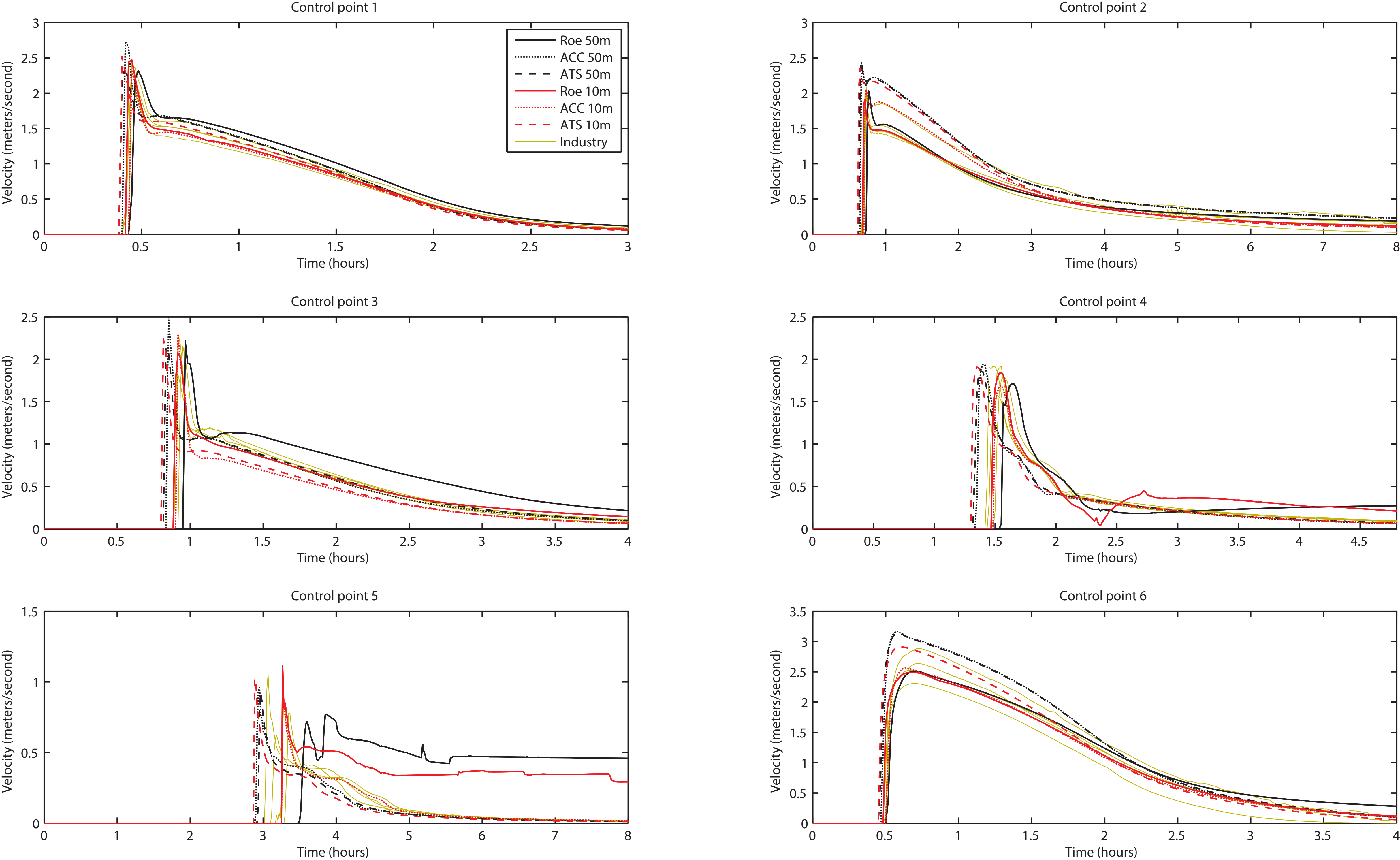

Control point 1
Control point 2
Control point 3
Control point 4
Control point 5
Control point 6
Velocity (meters/second)
Time (hours)
Roe 50m
ACC 50m
ATS 50m
Roe 10m
ACC 10m
ATS 10m
Industry

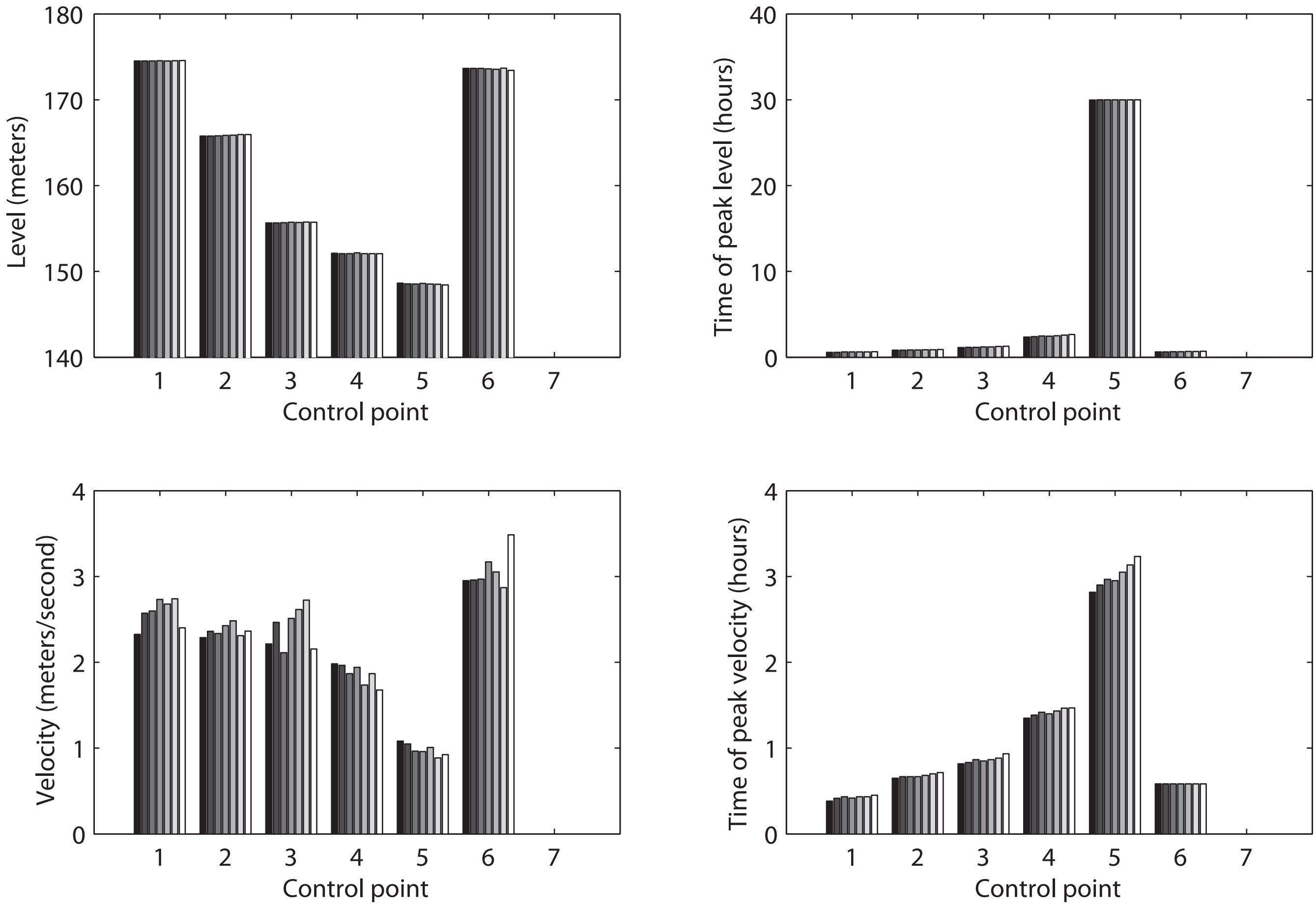

Level (meters)
180
170
160
150
140
1 2 3 4 5 6 7
Control point
Time of peak level (hours)
40
30
20
10
0
1 2 3 4 5 6 7
Control point
Velocity (meters/second)
4
3
2
1
0
1 2 3 4 5 6 7
Control point
Time of peak velocity (hours)
4
3
2
1
0
1 2 3 4 5 6 7
Control point

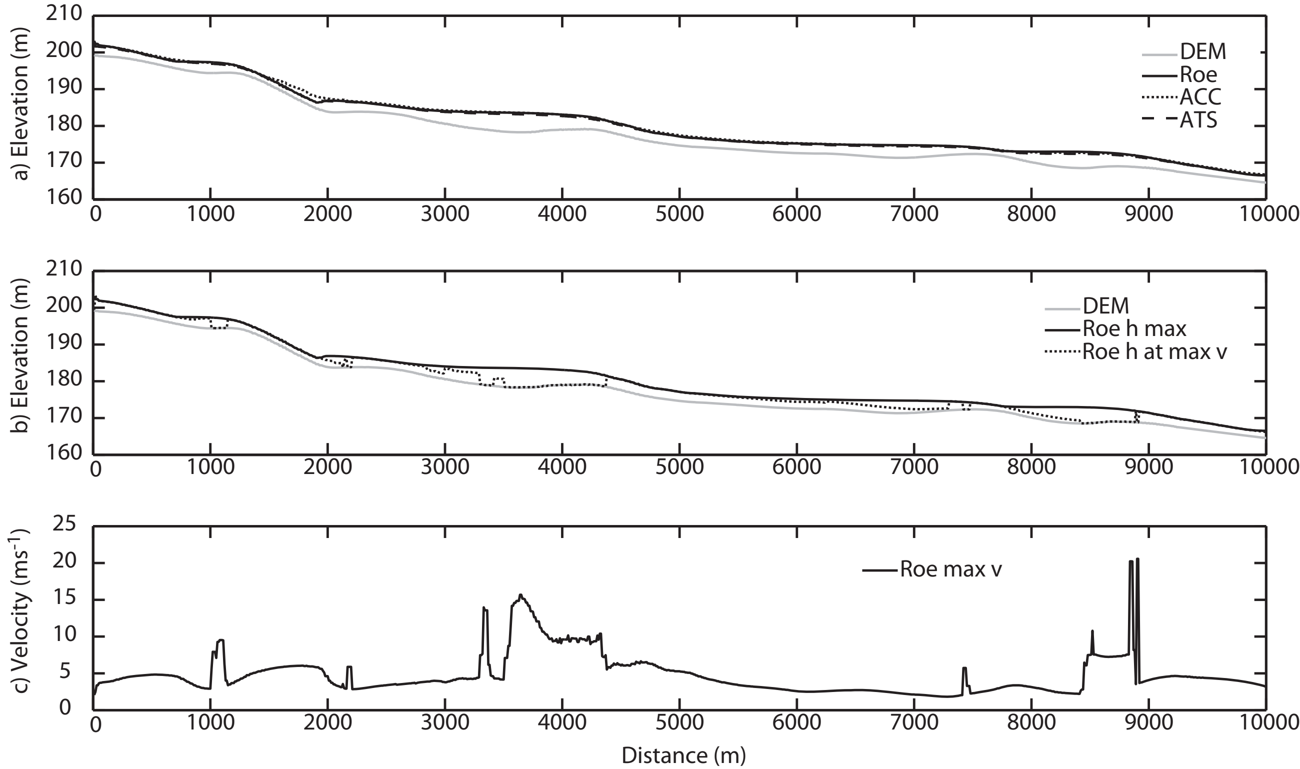
210
200
190
180
170
160
a) Elevation (m)
0
1000
2000
3000
4000
5000
6000
7000
8000
9000
10000
DEM
Roe
ACC
ATS
b) Elevation (m)
DEM
Roe h max
Roe h at max v
25
20
15
10
5
c) Velocity (ms-1)
Roe max v
Distance (m)

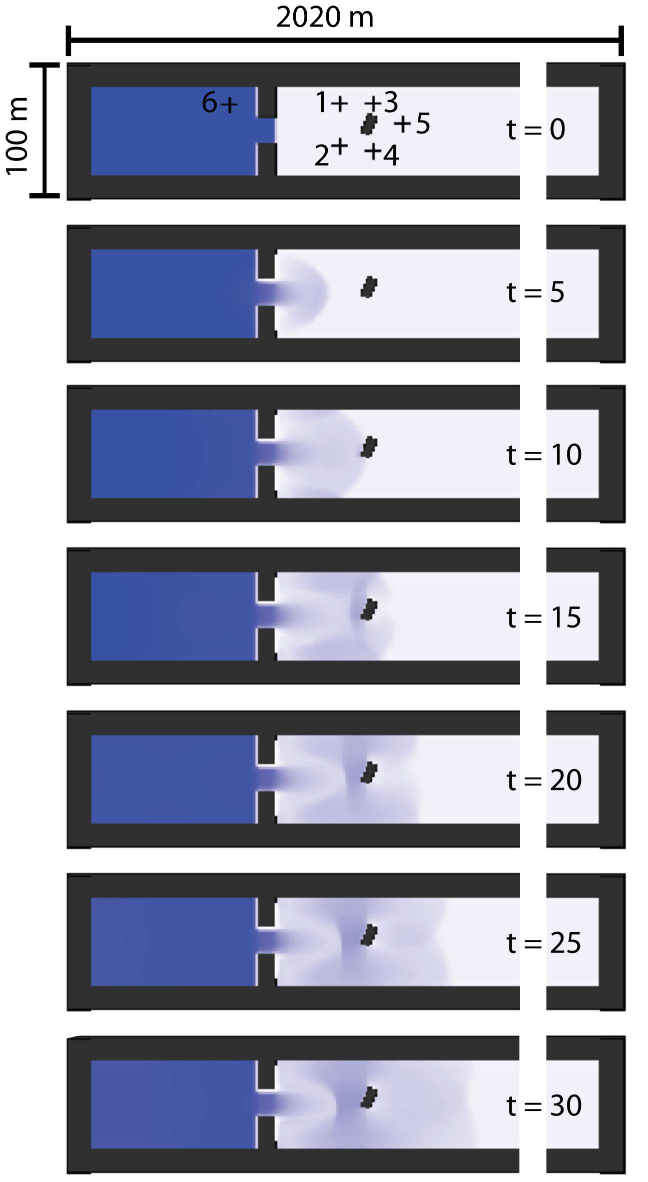
2020 m
100 m
6+
1+
+3
+5
2+
+4
t = 0
t = 5
t = 10
t = 15
t = 20
t = 25
t = 30

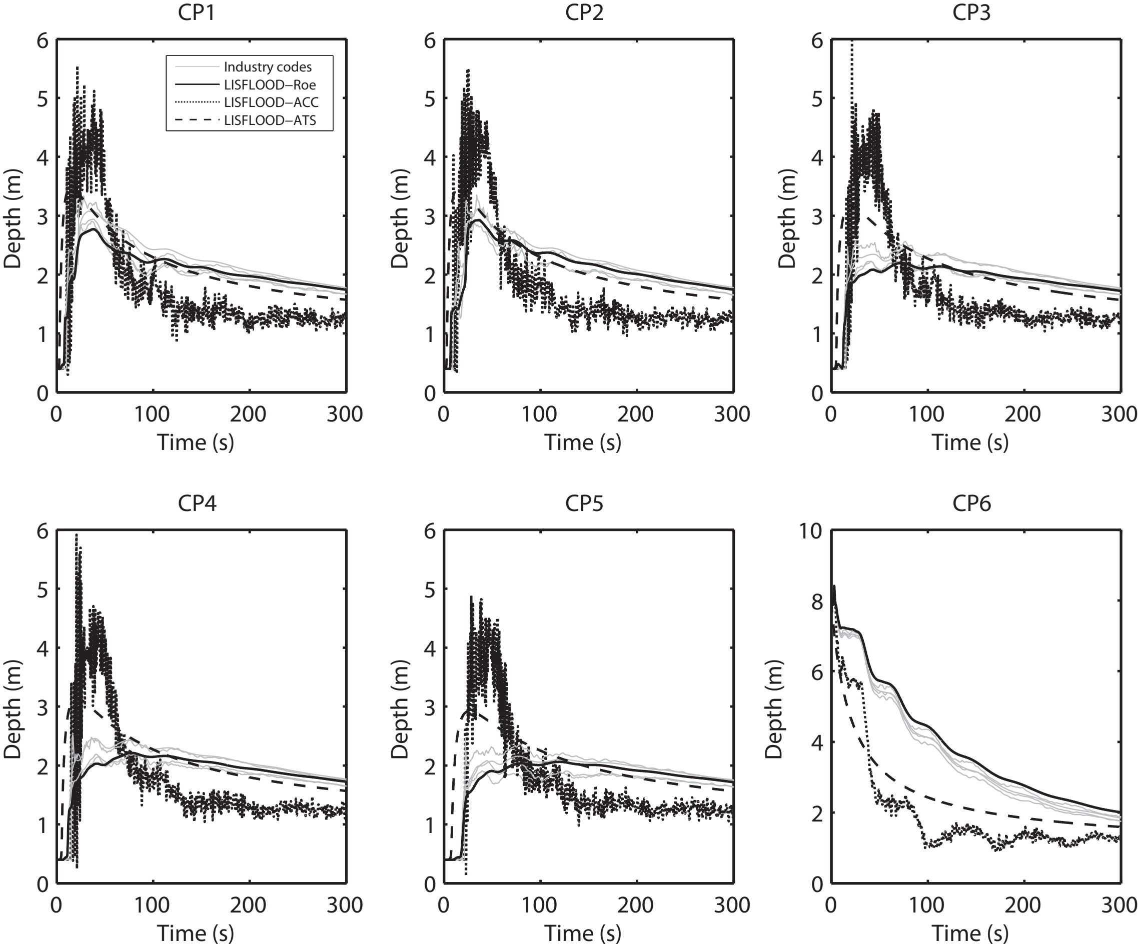

CP1
CP2
CP3
CP4
CP5
CP6
Industry codes
LISFLOOD−Roe
LISFLOOD−ACC
LISFLOOD−ATS
Depth (m)
Time (s)